

Increasing the *Brønsted* Acidity of Ph₂PO₂H by the Lewis Acid B(C₆F₅)₃. Formation of an Eight-Membered Boraphosphinate Ring [Ph₂POB(C₆F₅)₂O]₂

Ralf Kather,^a Elena Rychagova,^b Paula Sanz Camacho,^c Sharon E. Ashbrook,^c J. Derek Woollins,^c Lars Robben,^a Enno Lork,^a Sergey Ketkov,^{b,d*} Jens Beckmann^{a*}

^a Institut of Inorganic Chemistry and Crystallography, Bremen University, Leobener Straße, 28359 Bremen, Germany.

^b G.A.Razuvaev Institute of Organometallic Chemistry RAS, 49 Tropinin St., 603950 Nizhny Novgorod, Russian Federation

^c EaStChem. School of Chemistry, University of St. Andrews, St. Andrews, Fife KY16 9ST, United Kingdom

^d N. I. Lobachevsky Nizhny Novgorod State University, Gagarin ave. 23, 603950 Nizhny Novgorod, Russian Federation

Supplementary Information

Content

Experimental section

NMR spectra

X-ray crystallography

X-ray powder diffraction

Computational details

Additional references

Experimental Section

General Procedures. Diphenylphosphinic acid (Acros Organics, GB), Silicon Grease (Wacker Chemie AG, Burghausen, Germany), Tetraphenyltin, 15-crown-5 (Alfa Aesar, Germany) and Dimethyltin oxide (Sigma Aldrich, USA) were obtained commercially and used as received. Tris(pentafluorophenyl)borane was prepared according to literature procedures.^[S1] Dry toluene, dichloromethane and *n*-hexane were collected from a SPS800 mBraun solvent system.

Solution NMR spectroscopy. ^1H -, ^{13}C -, ^{11}B -, ^{19}F -, ^{29}Si -, ^{31}P - and ^{119}Sn -NMR spectra were recorded in CDCl_3 or $\text{THF}-d_8$ at r.t. using a Bruker Avance-360 spectrometer and are referenced to tetramethylsilane (^1H , ^{13}C , ^{29}Si), boron trifluoride diethyl etherate (^{11}B), trichlorofluoromethane (^{19}F), phosphoric acid (85% in water) (^{31}P) and tetramethyltin (^{119}Sn). Chemical shifts are reported in parts per million (ppm) and coupling constants (J) are given in hertz (Hz).

Solid-state NMR spectroscopy. ^{31}P and ^{119}Sn Solid-state NMR spectra were performed using Bruker Avance III spectrometers operating at magnetic field strength of 9.4 T, corresponding to Larmor frequencies of 161.9 and 149.2 MHz. Experiments were carried out using conventional 4-mm MAS probes, with 14 kHz MAS rate. Chemical shifts are referenced to 85% H_3PO_4 at 0 ppm using the isotropic resonance of solid BPO_4 at -29.6 ppm and to $(\text{CH}_3)_4\text{Sn}$ at 0 ppm using the isotropic resonance of solid SnO_2 at -604.3 ppm as a secondary reference respectively. For ^{31}P , NMR spectra were acquired using a $\pi/2$ pulse lengths of 2.6 μs , with 32 transients and a recycle interval of 5 s. For ^{119}Sn , NMR spectra were acquired using a $\pi/2$ pulse lengths of 1.6 μs , with 3072 transients and a recycle interval of 20 s. In both cases, continuous wave (cw) ^1H decoupling were applied during acquisition. For all spectra, the positions of isotropic resonances within the spinning sideband patterns were unambiguously determined by recording a second spectrum at a higher MAS rate. The ^{119}Sn MAS NMR spectrum was obtained from a partly decomposed sample that was stored for 3 month under inert conditions prior to the data acquisition. The signal at $\delta_{\text{iso}} = 70$ ppm is indicative for the unassigned decomposition product that also occurs in solution.

IR spectroscopy. IR spectra were recorded on a Perkin Elmer Spectrum 1000 FT-IR spectrometer as KBr discs and are reported in cm^{-1} .

Mass spectrometry. Electron impact mass spectroscopy (EIMS) was carried out using a Finnigan MAT 95. The ESI MS spectra were obtained with a Bruker Esquire-LC MS instrument. Acetonitrile or dichloromethane/acetonitrile (1:10) solution $c = 1 \cdot 10^{-5}$ mol · L⁻¹ were injected directly into the spectrometer at a flow rate of 3 µL · min⁻¹ and a pressure of 5 psi. Pressure in the mass analyzer region was usually about $1 \cdot 10^{-5}$ mbar. Spectra were collected for 1 min and averaged.

Microanalysis and Melting points. Elemental analyses (C, H) were carried out by IWR, TU Wien, Austria using a Elementar Vario Macro. The carbon percentage of **2** and **3** is lower than expected, which has been attributed to incomplete combustion. This observation has been made previously for compounds containing $[B(C_6F_5)_4]^-$ ions.^[S2] The melting points were determined using a Gallenkamp Melting Point Apparatus.

NMR scale formation of Ph₂P(OH)OB(C₆F₅)₃ (1). For the characterization of **1**, tris(pentafluorophenyl)borane (30.0 mg, 0.06 mmol) and diphenylphosphinic acid (12.8 mg, 0.06 mmol) were solved in 500 µl CDCl₃. The clear solution was measured immediately and showed signals of **1** only.

¹H-NMR (CDCl₃): δ = 7.76-7.38 (m, 10H, CH), 6.27 (br, 1H, OH). **¹³C{¹H}-NMR (CDCl₃):** δ = 147.9 (d, ¹J(¹⁹F-¹³C) = 243 Hz, CF), 139.9 (d, ¹J(¹⁹F-¹³C) = 255 Hz, CF), 137.5 (d, ¹J(¹⁹F-¹³C) = 224 Hz, CF), 134.8 (s, *p*-CH), 131.7 (d, ²J(³¹P-¹³C) = 13 Hz, *o*-CH), 129.3 (d, ³J(³¹P-¹³C) = 15 Hz, *m*-CH), 125.3 (d, ¹J(³¹P-¹³C) = 147 Hz, *i*-C). **¹¹B{¹H}-NMR (CDCl₃):** δ = -1.3 (br). **¹⁹F{¹H}-NMR (CDCl₃):** δ = -134.2 (m, 2F, *o*-C₆F₅), -160.8 (tr, ³J(¹⁹F-¹⁹F) = 20 Hz, 1F, *p*-C₆F₅), -166.3 (m, 2F, *m*-C₆F₅). **³¹P{¹H}-NMR (CDCl₃):** δ = 42.1 (s, ¹J(¹³C-³¹P) = 147 Hz).

Synthesis of [Na(15-crown-5)] [Ph₂P(O)OB(C₆F₅)₃] (2). Sodium diphenylphosphinate was prepared by adding sodium methoxide (25.0 mg, 0.463 mmol) to diphenylphosphinic acid (100 mg, 0.458) in methanol and stirring overnight. The solvent was removed and the sodium diphenylphosphinate was used as obtained. Tris(pentafluorophenyl)borane (173 mg, 0.338 mmol), sodium diphenylphosphinate (81.2 mg, 0.338 mmol) and 15-crown-5 (74.5 mg, 0.338 mmol) stirred in toluene for 12 h at room temperature. The solvent was removed and the residue was washed with *n*-hexane and recrystallized from dichloromethane and *n*-hexane to give **2** as colourless crystals (241 mg, 0.248 mmol, 73 %; Mp. 209 °C (dec)).

¹H-NMR (THF-d₈): δ = 7.82-7.58 (m, 4H, CH), 7.41-7.20 (m, 6H, CH), 3.57 (s, 20H, CH₂). **¹³C{¹H}-NMR (THF-d₈):** δ = 146.5 (d, ¹J(¹⁹F-¹³C) = 242 Hz, CF), 137.3 (d, ¹J(¹⁹F-¹³C) = 245 Hz, CF), 135.0 (d, ¹J(¹⁹F-¹³C) = 242 Hz, CF), 134.6 (d, ¹J(³¹P-¹³C) = 143 Hz, *i*-C), 129.7 (d, ²J(³¹P-¹³C) = 10 Hz, *o*-CH), 128.7 (d, ⁴J(³¹P-¹³C) = 2 Hz, *p*-CH), 125.8 (d, ³J(³¹P-¹³C) = 13 Hz, *m*-CH), 67.5 (s, CH₂). **¹¹B{¹H}-NMR (THF-d₈):** δ = -2.7 (br). **¹⁹F{¹H}-NMR (THF-d₈):** δ = -133.3 (m, 2F, *o*-C₆F₅), -165.1 (tr, ³J(¹⁹F-¹⁹F) = 20 Hz, 1F, *p*-C₆F₅), -168.8 (m, 2F, *m*-C₆F₅). **³¹P{¹H}-NMR (THF-d₈):** δ = 22.3 (s, ¹J (¹³C-³¹P) = 143 Hz). **MS (ESI, negative Modus, CH₃CN):** *m/z* = 728.9 [Ph₂P(O)OB(C₆F₅)₃]⁻. **IR (KBr, cm⁻¹):** ν = 2912 (s), 2874 (s), 1642 (m), 1514 (s), 1465 (s), 1355 (m), 1278 (m), 1246 (m), 1224 (m), 1119 (s), 1087 (s), 972 (s), 943 (s), 854 (w), 764 (m), 725 (m), 683 (m), 556 (m), 528 (m). Anal. Calcd for C₄₀H₃₀BF₂₀NaO₇P: C, 49.41; H, 3.11. Found: C, 48.32; H, 2.99 (see comment above).

Synthesis of [Ph₂POB(C₆F₅)₂O]₂ (3). Tris(pentafluorophenyl)borane (235 mg, 0.460 mmol) and diphenylphosphinic acid (100 mg, 0.460 mmol) stirred in 15 ml toluene under reflux overnight. After cooling to room temperature the solvent was removed by rotary evaporation affording a colourless solid which was solved in dichloromethane, filtered through silicia gel and recrystallized from dichloromethane and *n*-hexane to give **3** as colourless crystals (196 mg, 0.174 mmol, 76 %; Mp. 227-229 °C).

¹H-NMR (CDCl₃): δ = 7.70-7.56 (m, 12H, CH), 7.44-7.34 (m, 8H, CH). **¹³C{¹H}-NMR (CDCl₃):** δ = 147.3 (d, ¹J(¹⁹F-¹³C) = 248 Hz, CF), 140.1 (d, ¹J(¹⁹F-¹³C) = 251 Hz, CF), 137.1 (d, ¹J(¹⁹F-¹³C) = 237 Hz, CF), 134.2 (d, ⁴J(³¹P-¹³C) = 2 Hz, *p*-CH), 132.1 (d, ²J(³¹P-¹³C) = 13 Hz, *o*-CH), 128.5 (d, ³J(³¹P-¹³C) = 15 Hz, *m*-CH), 125.4 (d, ¹J(³¹P-¹³C) = 148 Hz, *i*-C). **¹¹B{¹H}-NMR (CDCl₃):** δ = 6.3 (br). **¹⁹F{¹H}-NMR (CDCl₃):** δ = -135.9 (m, 2F, *o*-C₆F₅), -158.5 (tr, ³J(¹⁹F-¹⁹F) = 20 Hz, 1F, *p*-C₆F₅), -165.4 (m, 2F, *m*-C₆F₅). **³¹P{¹H}-NMR (CDCl₃):** δ = 37.8 (s, ¹J (¹³C-³¹P) = 148 Hz). **MS (EI⁺):** *m/z* = 1124 [M]⁺, 957 [M-C₆F₅]⁺, 395 [M-(C₆F₅)₂]²⁺. **IR (KBr, cm⁻¹):** ν = 1648 (m), 1594 (w), 1518 (s), 1474 (s), 1385 (w), 1291 (m), 1262 (w), 1128 (s), 1041 (s), 1022 (s), 995 (m), 977 (m), 860 (m), 787 (m), 755 (m), 691 (m), 546 (m), 524 (s). Anal. Calcd for C₄₈H₂₀B₂F₂₀O₄P₂: C, 51.28; H, 1.79. Found: C, 49.08; H, 1.85 (see comment above).

Synthesis of $[\text{Ph}_2\text{P}(\text{O})\text{OSi}(\text{Me})_2]_2\text{O} \cdot [\text{H}_2\text{OB}(\text{C}_6\text{F}_5)]_2$ (4). Tris(pentafluorophenyl)borane (200 mg, 0.391 mmol), diphenylphosphinic acid (85.3 mg, 0.391 mmol) and “Silicon Grease” ($\text{HO}[\text{Me}_2\text{SiO}]_n\text{H}$, 512 mg) were stirred under moisture in 10 ml toluene at room temperature for three days. The solvent was removed by rotary evaporation. The crude product was washed three times with hot *n*-hexane and recrystallized from dichloromethane and *n*-hexane to obtain **4** as colourless solid (194 mg, traces of silicon grease still present).

$^1\text{H-NMR}$ (THF-*d*₈): $\delta = 8.10$ (s (broad), 4H, BOH₂), 7.75-7.60 (m, 8H, CH), 7.54-7.39 (m, 12H, CH), 1.30 (s, silicon grease), 0.12 (s, silicon grease), 0.10 (s, 12H, CH₂). **$^{13}\text{C}\{\text{H}\}$ -NMR (THF-*d*₈):** $\delta = 149.2$ (d, $^1J(^{19}\text{F}-^{13}\text{C}) = 241$ Hz, CF), 140.8 (d, $^1J(^{19}\text{F}-^{13}\text{C}) = 249$ Hz, CF), 137.9 (d, $^1J(^{19}\text{F}-^{13}\text{C}) = 249$ Hz, CF), 134.0 (d, $^1J(^{31}\text{P}-^{13}\text{C}) = 140$ Hz, *i*-C), 132.9 (d, $^4J(^{31}\text{P}-^{13}\text{C}) = 1$ Hz, *p*-CH), 132.1 (d, $^2J(^{31}\text{P}-^{13}\text{C}) = 10$ Hz, *o*-CH), 129.3 (d, $^3J(^{31}\text{P}-^{13}\text{C}) = 13$ Hz, *m*-CH), 30.7 (s, silicon grease), 1.4 (s, silicon grease), 0.9 (s, CH₃). **$^{11}\text{B}\{\text{H}\}$ -NMR (THF-*d*₈):** $\delta = 3.4$ (br). **$^{19}\text{F}\{\text{H}\}$ -NMR (THF-*d*₈):** $\delta = -132.5$ (m, 2F, *o*-C₆F₅), -157.5 (tr, $^3J(^{19}\text{F}-^{19}\text{F}) = 20$ Hz, 1F, *p*-C₆F₅), -163.8 (m, 2F, *m*-C₆F₅). **$^{29}\text{Si}\{\text{H}\}$ -NMR (THF-*d*₈):** $\delta = -21.1$ (s, silicon grease), -23.9 (s, SiMe₂). **$^{31}\text{P}\{\text{H}\}$ -NMR (THF-*d*₈):** $\delta = 32.4$ (s, $^1J(^{13}\text{C}-^{31}\text{P}) = 140$ Hz). **IR (KBr, cm⁻¹):** $\nu = 3429$ (broad), 2357 (w), 2338 (w), 1646 (m), 1518 (s), 1468 (s), 1377 (w), 1285 (m), 1265 (m), 1138 (s), 1098 (s), 975 (m), 813 (m), 692 (m), 544 (m).

Synthesis of $[\text{Me}_2\text{Sn}(\text{OPPh}_2\text{O})_2\text{SnMe}_2][\text{HOB}(\text{C}_6\text{F}_5)_3]_2$ (5). Tris(pentafluorophenyl)borane (250 mg, 0.488 mmol), diphenylphosphinic acid (107 mg, 0.488 mmol) and dimethyltin oxide (80,5 mg, 0.489 mmol) stirred in 5 ml dichloromethane at room temperature for 48 hours. The solution was concentrated and layered with *n*-hexane. The precipitate was dried under vacuum to obtain **5** as colourless solid (364 mg, 0.203 mmol, 83%; Mp. 85-88 °C).

^{31}P -MAS NMR: $\delta = 31.2$ (s). **^{119}Sn -MAS-NMR:** $\delta = -180.5$ (s). **$^{31}\text{P}\{\text{H}\}$ -NMR (C₆D₆):** $\delta = 29.6$ (s, $^2J(^{119/117}\text{Sn}-\text{O}-^{31}\text{P}) = 134$ Hz), 28.2 (s, $^2J(^{119/117}\text{Sn}-\text{O}-^{31}\text{P}) = 132$ Hz), 24.9 (s), 24.8 (s, $^2J(^{119/117}\text{Sn}-\text{O}-^{31}\text{P}) = 161$ Hz). **$^{119}\text{Sn}\{\text{H}\}$ -NMR (C₆D₆):** $\delta = -217.1$ (d, $^2J(^{31}\text{P}-\text{O}-^{119}\text{Sn}) = 139$ Hz), -218.9 (d, $^2J(^{31}\text{P}-\text{O}-^{119}\text{Sn}) = 142$ Hz). **MS (ESI, positive Modus, CH₂Cl₂/CH₃CN (1:10)): m/z = 528.9 [Me₂SnOP(Ph)₂OSnMe₂O]⁺.** **(ESI, negative Modus, CH₂Cl₂/CH₃CN (1:10)): m/z = 728.9 [Ph₂P(O)OB(C₆F₅)₃]⁻, 528.9 [HOB(C₆F₅)₃]⁻.** **IR (KBr, cm⁻¹):** $\nu = 3615$ (w), 3228 (w, broad), 1644 (m), 1592 (w), 1518 (s), 1466 (s), 1367 (w), 1284 (m), 1138 (s), 1089 (m), 1036 (m), 1017(m), 996 (m), 977 (m), 928 (w), 908 (w), 798 (m), 752 (m), 732 (m).

Synthesis of Ph₃SnOP(Ph₂)(O)B(C₆F₅)₃ (6**).** Tris(pentafluorophenyl)borane (250 mg, 0.488 mmol), diphenylphosphinic acid (107 mg, 0.488 mmol) and tetraphenyltin (209 mg, 0.488 mmol) stirred in toluene at room temperature for 4 days. The solvent was removed under vacuum to obtain crude product which was solved in dichloromethane and layered with *n*-hexane. The precipitate was dried under vacuum to give **6** as colourless solid (451 mg, 0.418 mmol, 86 %; Mp. 169-171 °C).

¹H-NMR (CDCl₃): δ = 7.50-7.18 (m, 25H, CH). **¹³C{¹H}-NMR (CDCl₃):** δ = 147.9 (d, ¹J(¹⁹F-¹³C) = 241 Hz, CF), 139.4 (d, ¹J(¹⁹F-¹³C) = 243 Hz, CF), 136.7 (d, ¹J(¹⁹F-¹³C) = 239 Hz, CF), 136.3 (s, ²J(¹¹⁹/¹¹⁷Sn-¹³C) = 49 Hz, *o*-CH_(Sn-phenyl)), 135.6 (s, *i*-C_(Sn-phenyl)), 133.1 (d, ⁴J(³¹P-¹³C) = 3 Hz, *p*-CH_(P-phenyl)), 131.6 (d, ²J(³¹P-¹³C) = 13 Hz, *o*-CH_(P-phenyl)), 131.4 (s, ⁴J(¹¹⁹/¹¹⁷Sn-¹³C) = 14 Hz, *p*-CH_(Sn-phenyl)), 129.6 (s, ³J(¹¹⁹/¹¹⁷Sn-¹³C) = 66 Hz, *m*-CH_(Sn-phenyl)), 128.7 d, ¹J(³¹P-¹³C) = 148 Hz, *i*-C_(P-phenyl)), 128.4 (d, ³J(³¹P-¹³C) = 15 Hz, *m*-CH_(P-phenyl)). **¹¹B{¹H}-NMR (CDCl₃):** δ = -1.9 (br). **¹⁹F{¹H}-NMR (CDCl₃):** δ = -134.4 (m, 2F, *o*-C₆F₅), -161.0 (tr, ³J(¹⁹F-¹⁹F) = 20 Hz, 1F, *p*-C₆F₅), -166.4 (m, 2F, *m*-C₆F₅).

³¹P{¹H}-NMR (CDCl₃): δ = 31.3 (s, ²J (¹¹⁹/¹¹⁷Sn-O-³¹P) = 143 Hz). **¹¹⁹Sn{¹H}-NMR (CDCl₃):** δ = -59.6 (d, ²J (³¹P -O-¹¹⁹Sn) = 146 Hz). **MS (EI⁺):** *m/z* = 568 [M-B(C₆F₅)₃]⁺, 512 [B(C₆F₅)₃]⁺, 491 [M-B(C₆F₅)₃-(C₆H₅)]⁺, 351 [(C₆H₅)₃Sn]⁺. **IR (KBr, cm⁻¹):** ν = 3062 (w), 1644 (m), 1590 (w), 1515 (s), 1466 (s), 1369 (w), 1284 (m), 1123 (s), 1058 (m), 1022 (w), 997 (m), 976 (m), 868 (w), 800 (w), 752 (m), 734 (s), 693 (s), 563 (m), 538 (m), 507 (w), 444 (w).

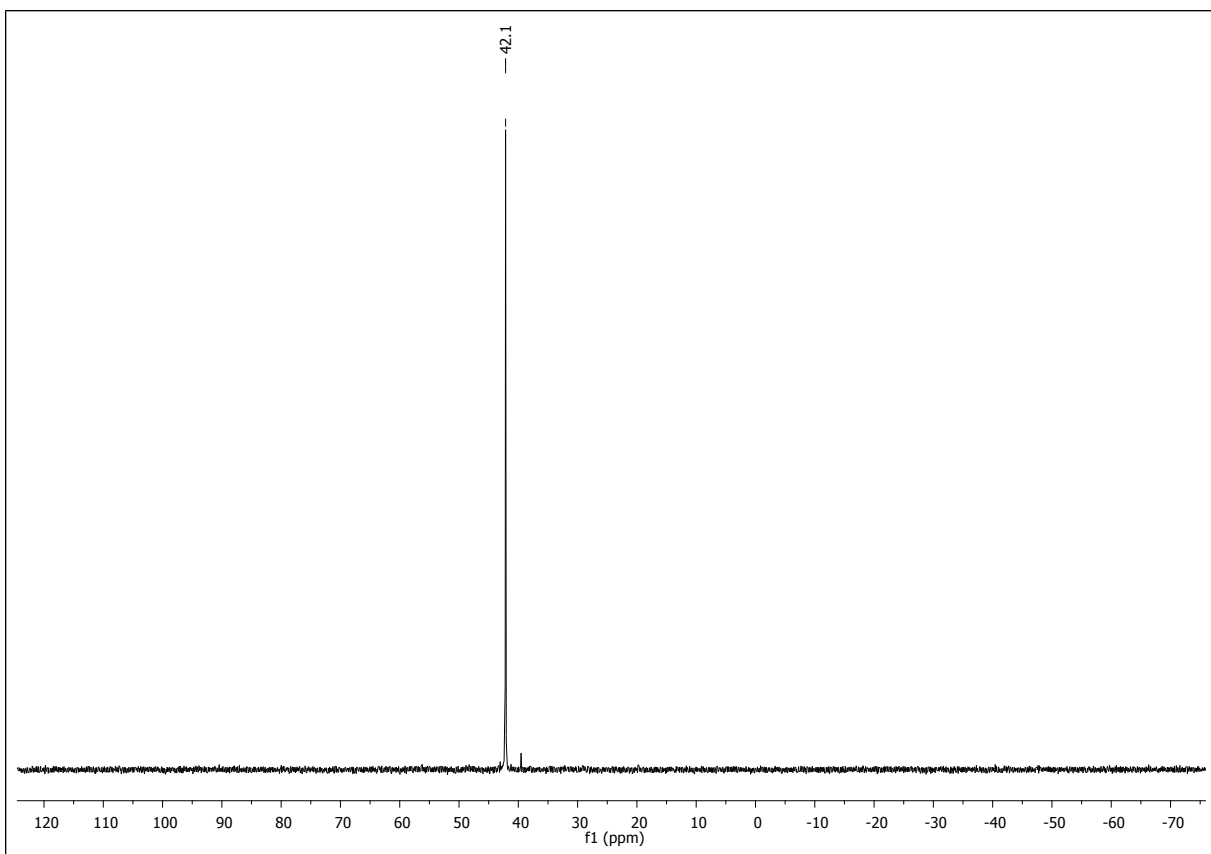


Figure S1. $^{31}\text{P}\{\text{H}\}$ -NMR of **1** (CDCl_3).

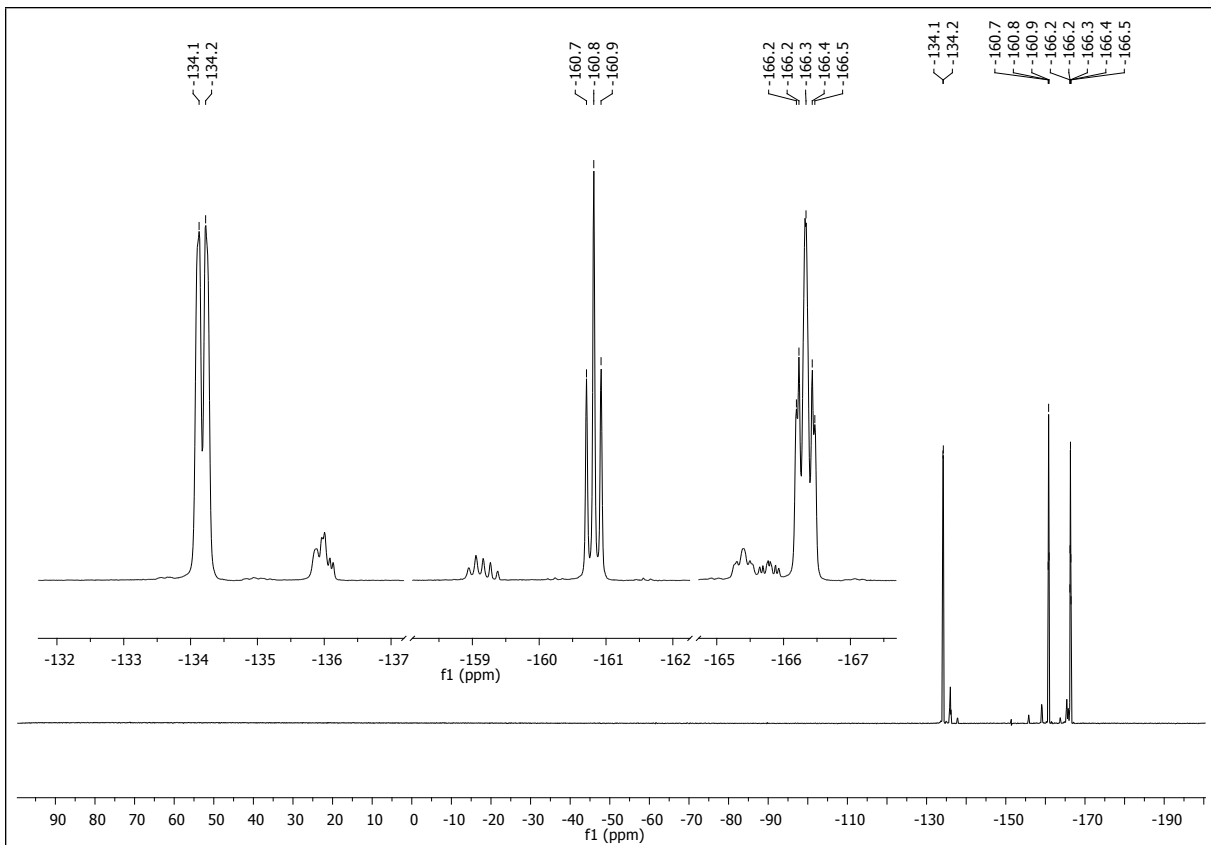


Figure S2. $^{19}\text{F}\{\text{H}\}$ -NMR of **1** (CDCl_3).

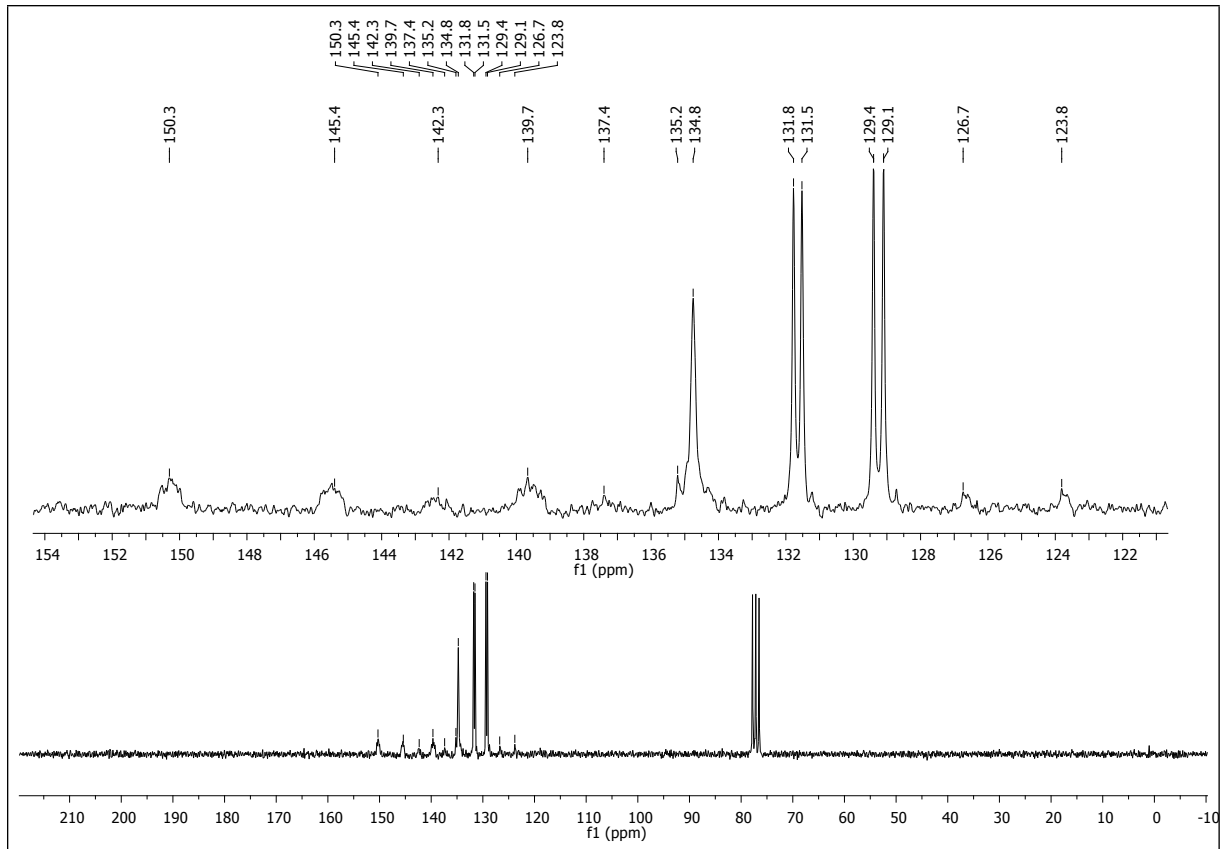


Figure S3. $^{13}\text{C}\{\text{H}\}$ -NMR of **1** (CDCl_3).

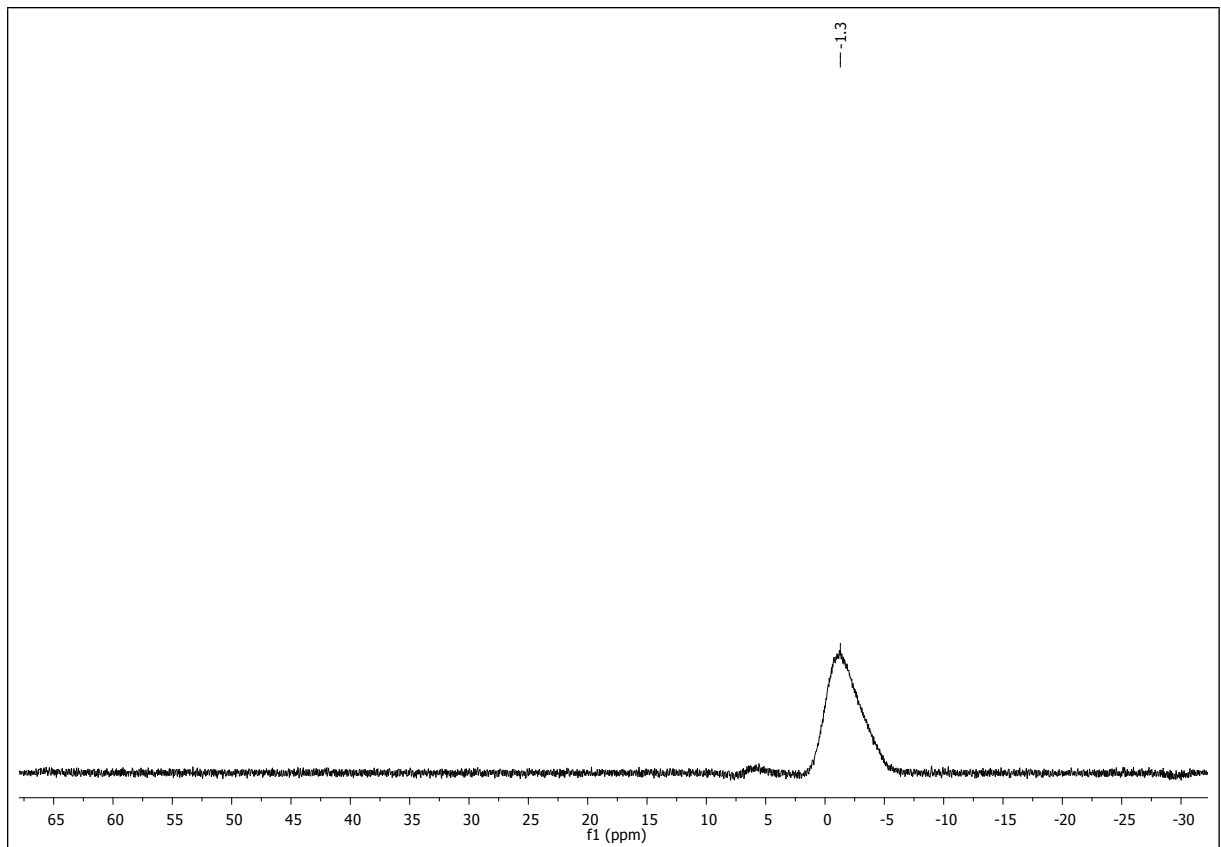


Figure S4. $^{11}\text{B}\{\text{H}\}$ -NMR of **1** (CDCl_3).

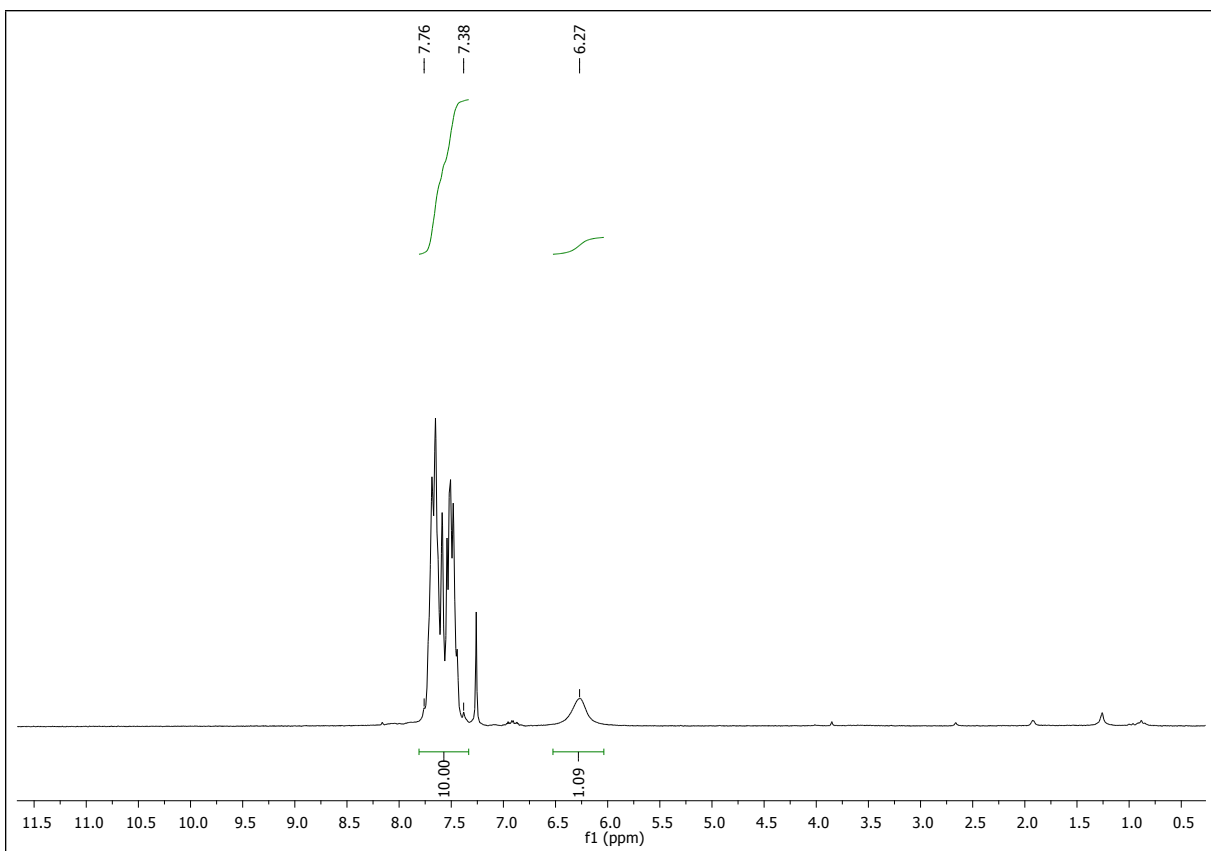


Figure S5. ^1H -NMR of **1** (CDCl_3).

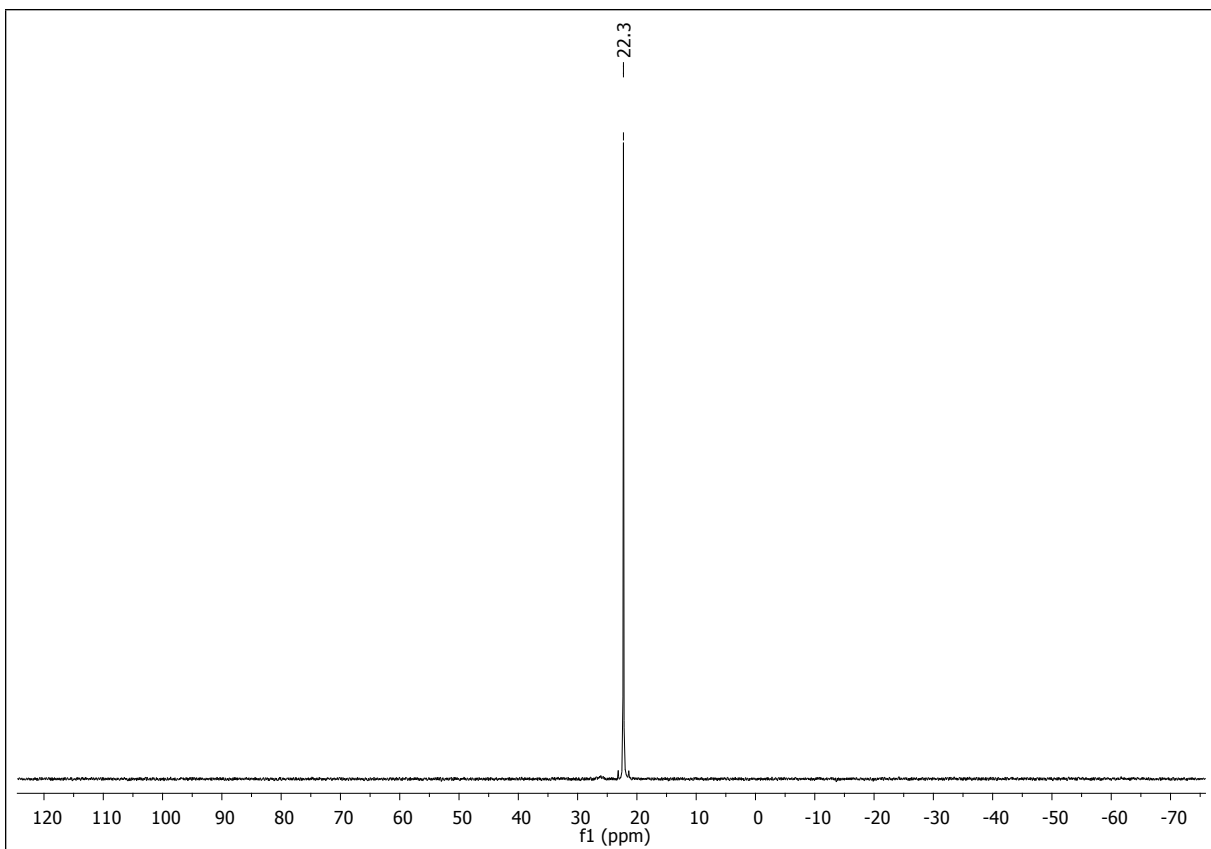


Figure S6. $^{31}\text{P}\{\text{H}\}$ -NMR of **2** ($\text{THF}-d_8$).

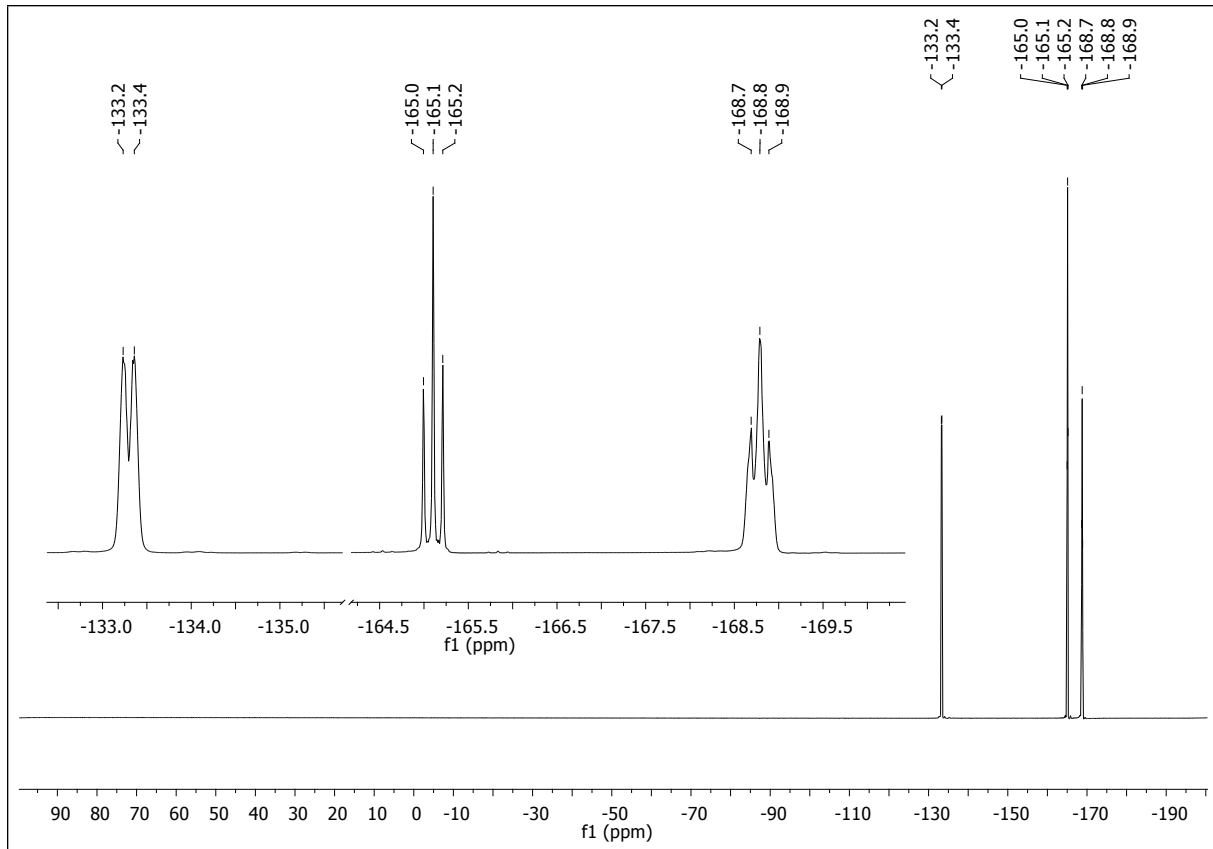


Figure S7. $^{19}\text{F}\{\text{H}\}$ -NMR of **2** (THF-*d*₈).

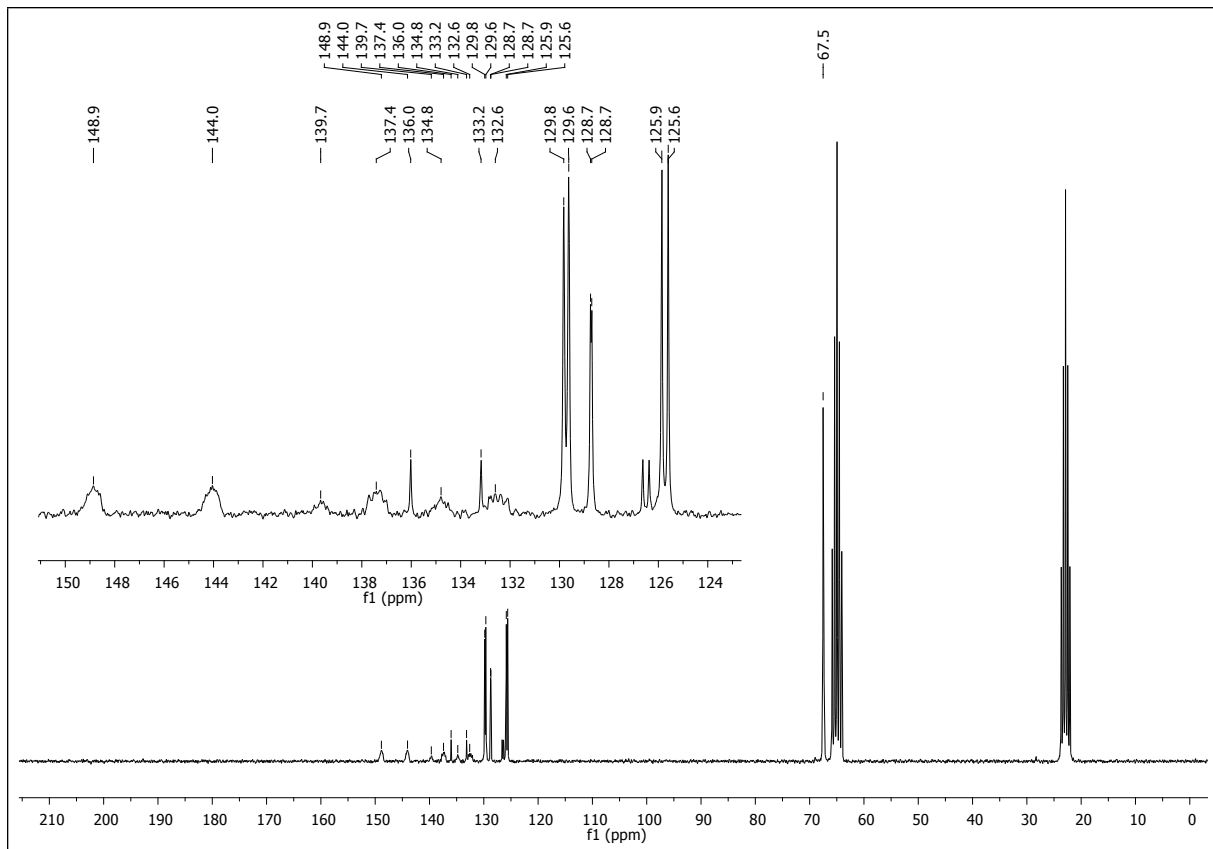


Figure S8. $^{13}\text{C}\{\text{H}\}$ -NMR of **2** (THF-*d*₈).

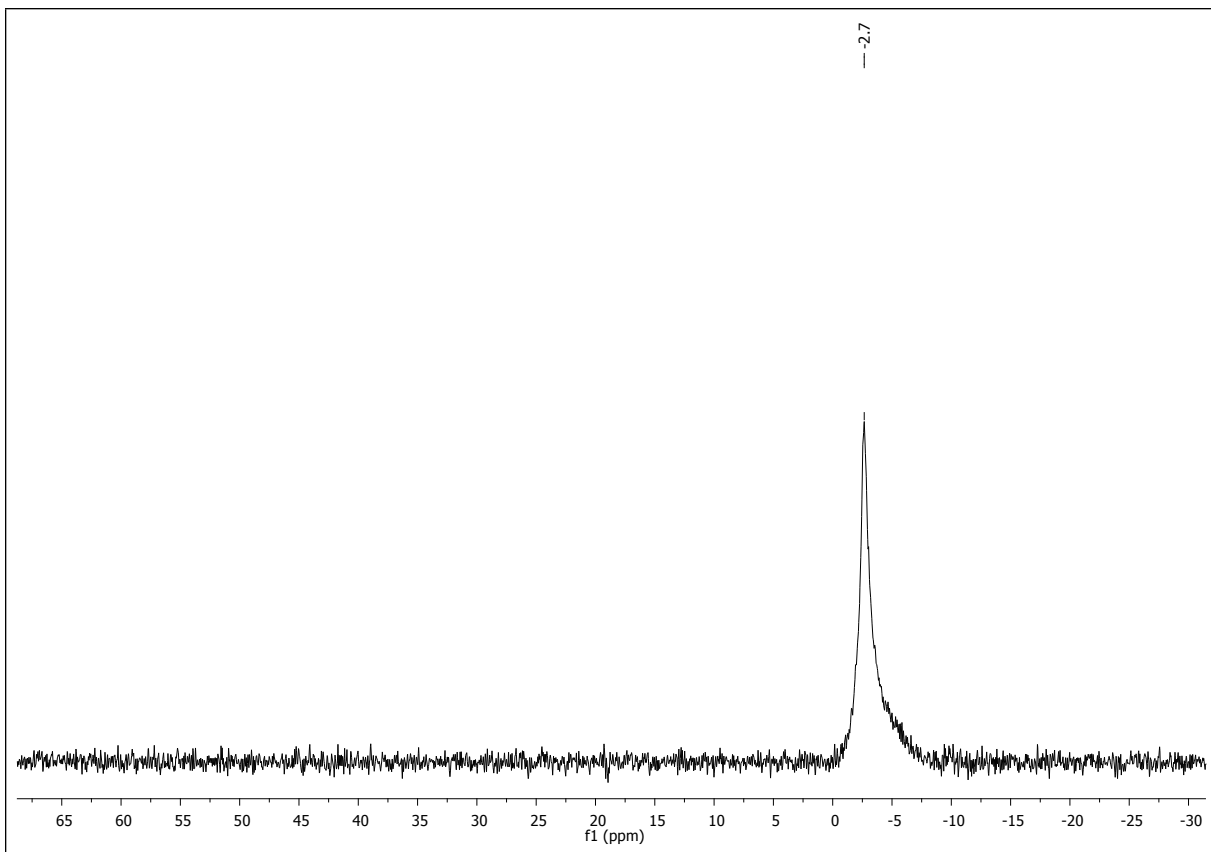


Figure S9. $^{11}\text{B}\{\text{H}\}$ -NMR of **2** (THF- d_8).

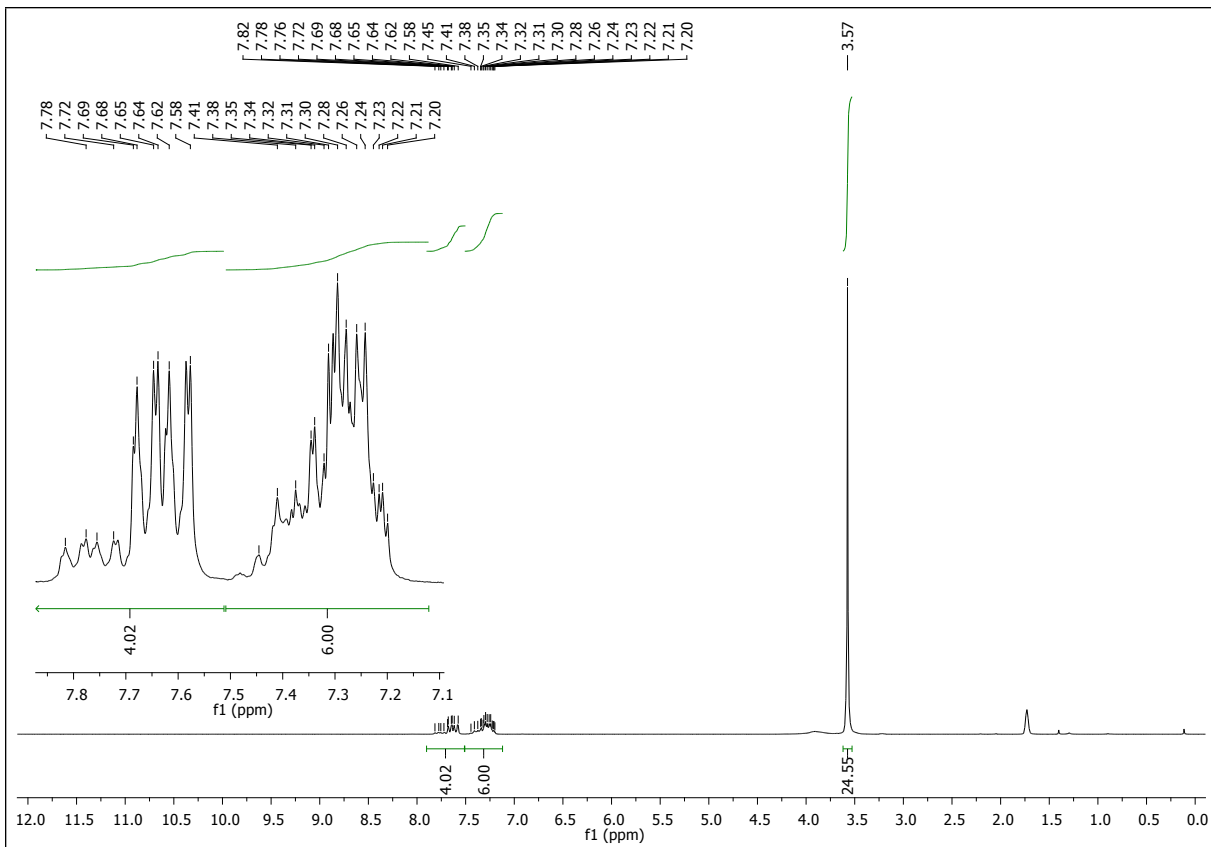


Figure S10. ^1H -NMR of **2** (THF- d_8).

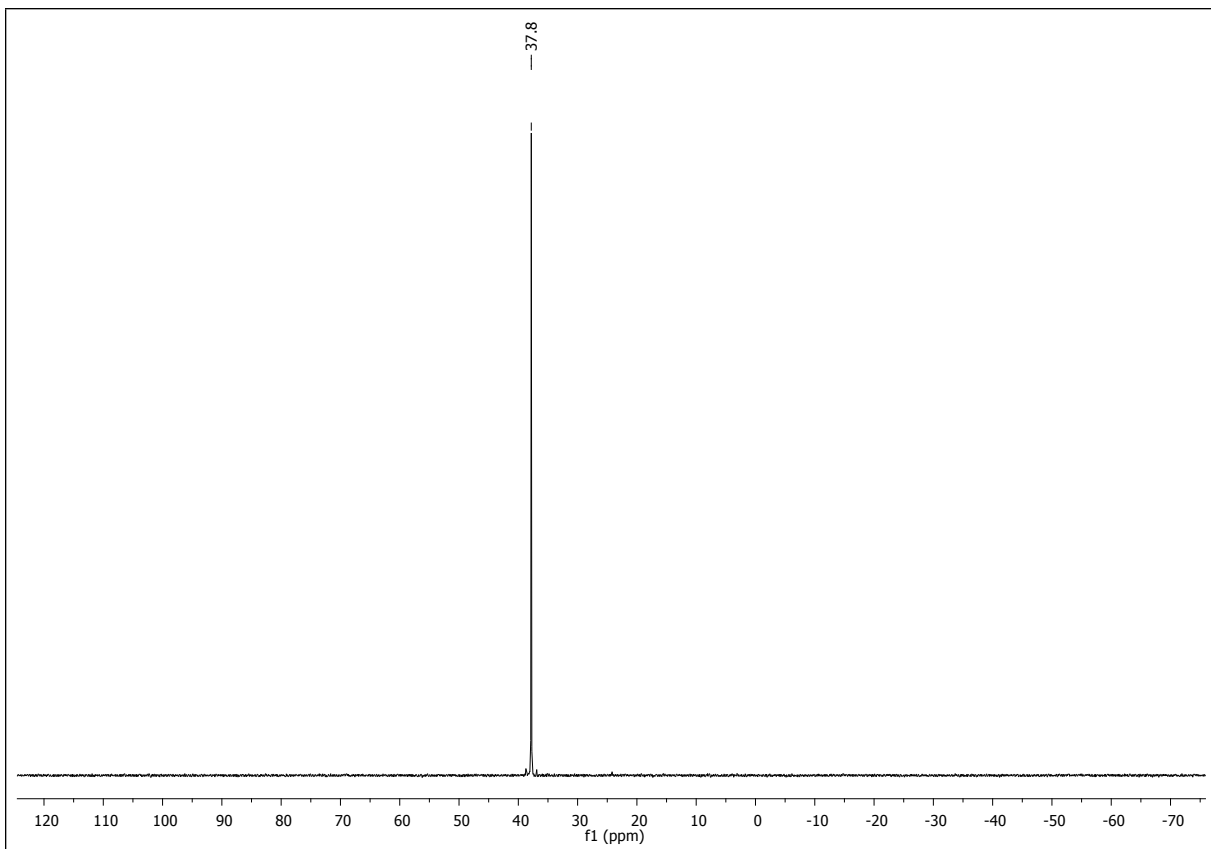


Figure S11. $^{31}\text{P}\{\text{H}\}$ -NMR of **3** (CDCl_3).

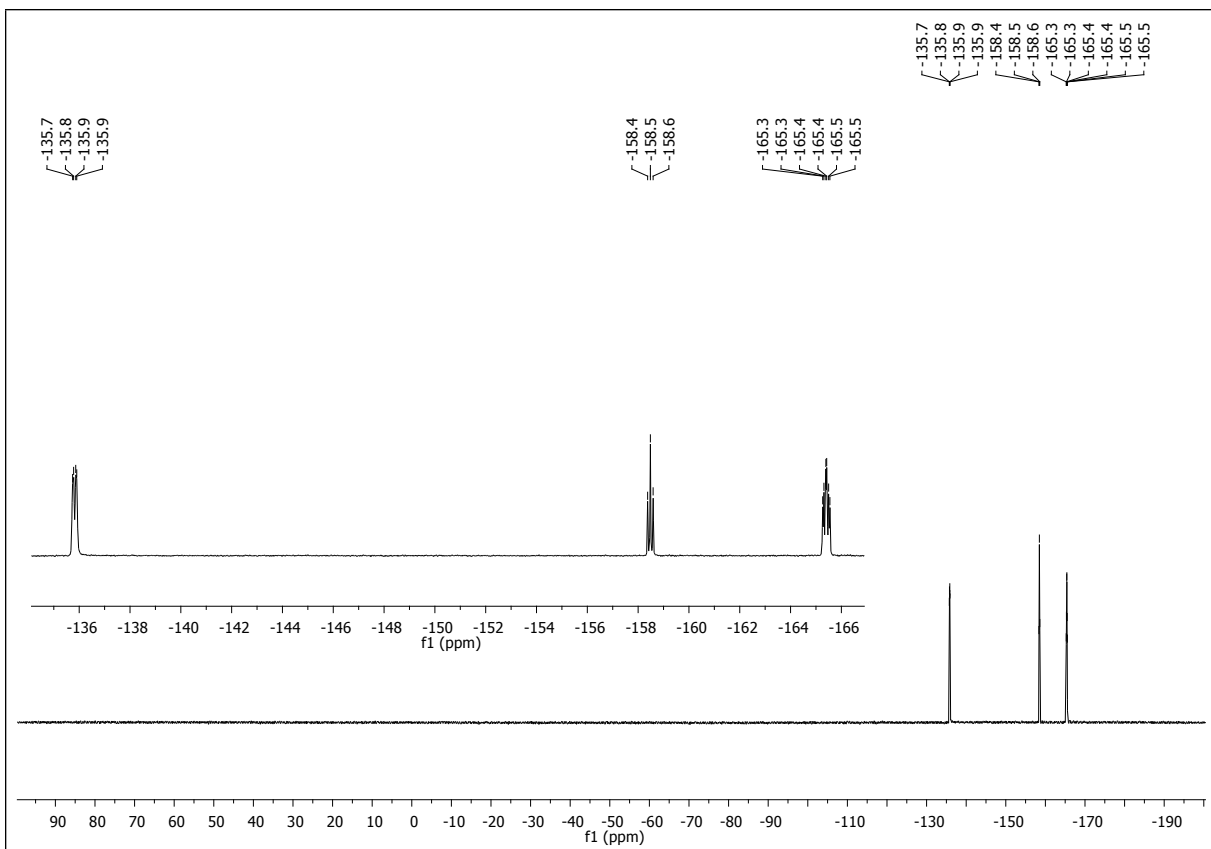


Figure S12. $^{19}\text{F}\{\text{H}\}$ -NMR of **3** (CDCl_3).

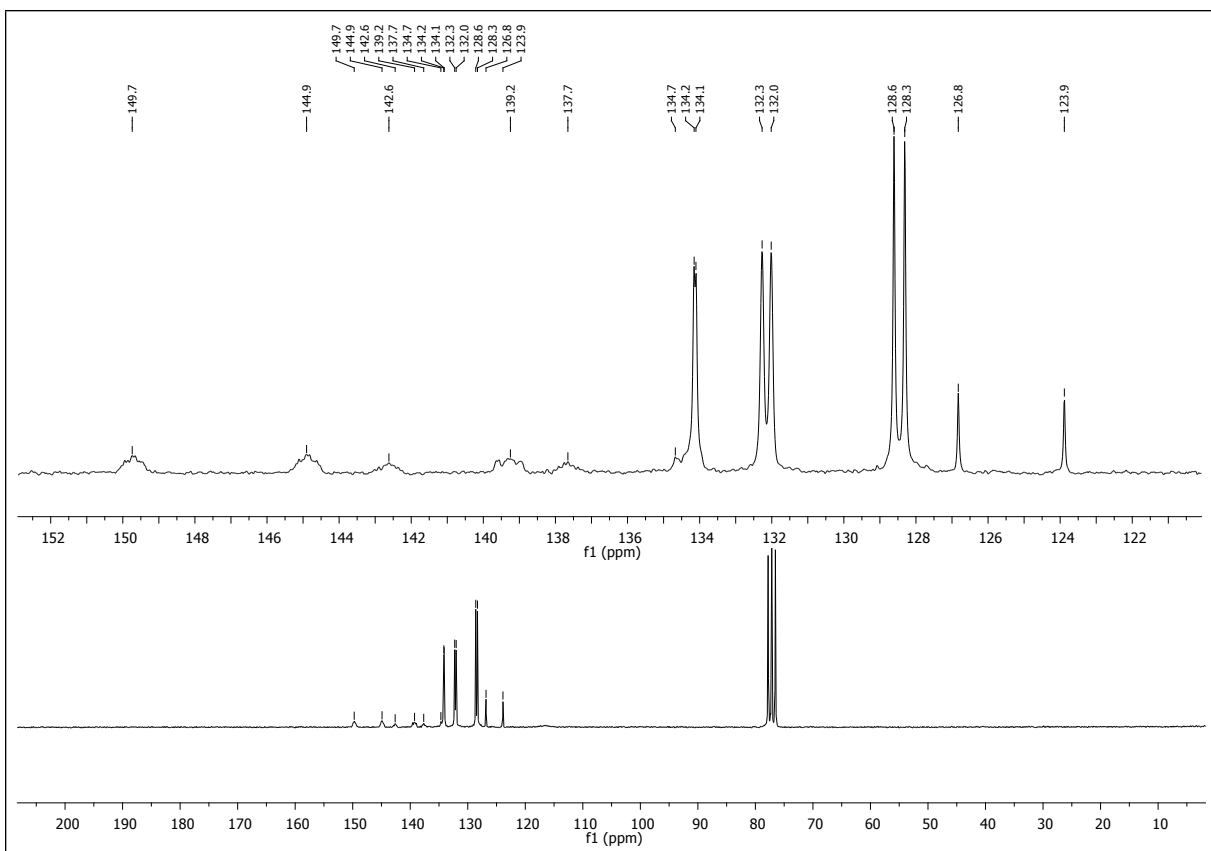


Figure S13. $^{13}\text{C}\{^1\text{H}\}$ -NMR of **3** (CDCl_3).

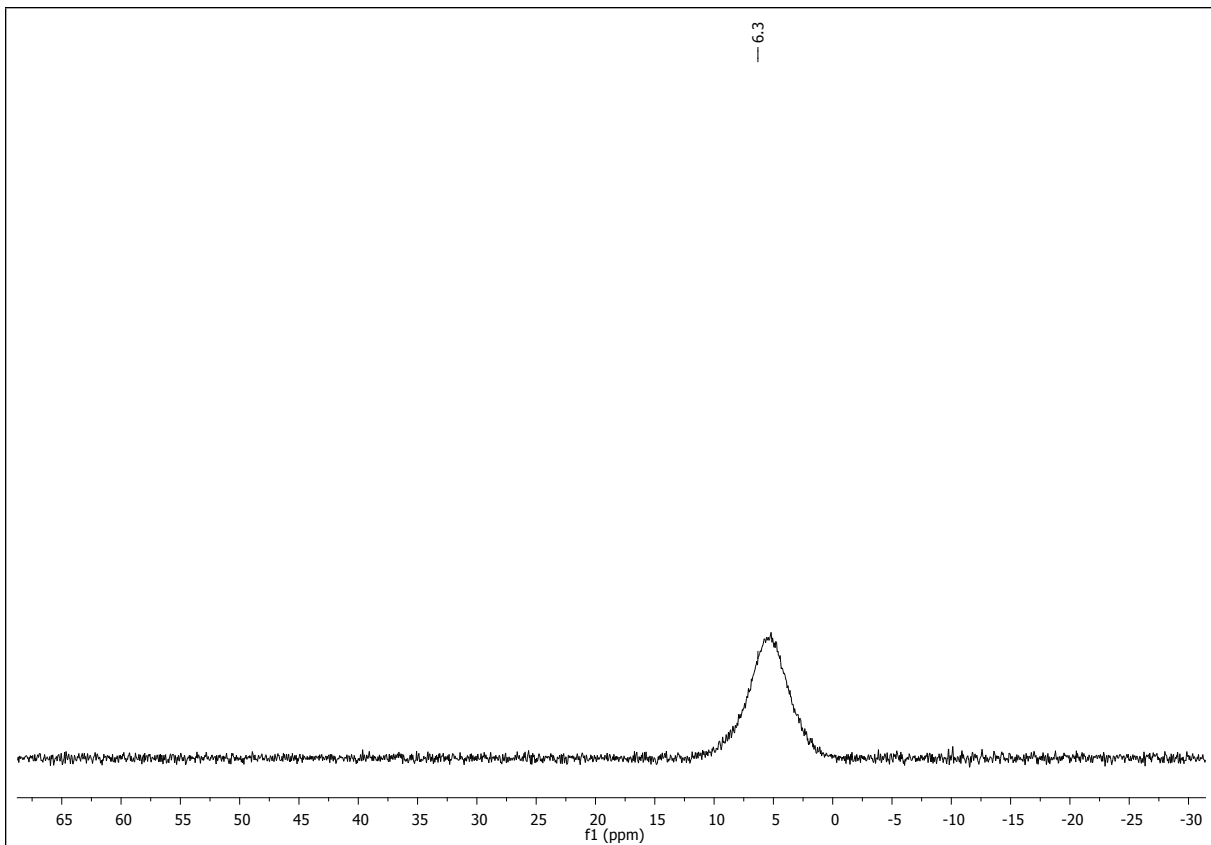


Figure S14. $^{11}\text{B}\{^1\text{H}\}$ -NMR of **3** (CDCl_3).

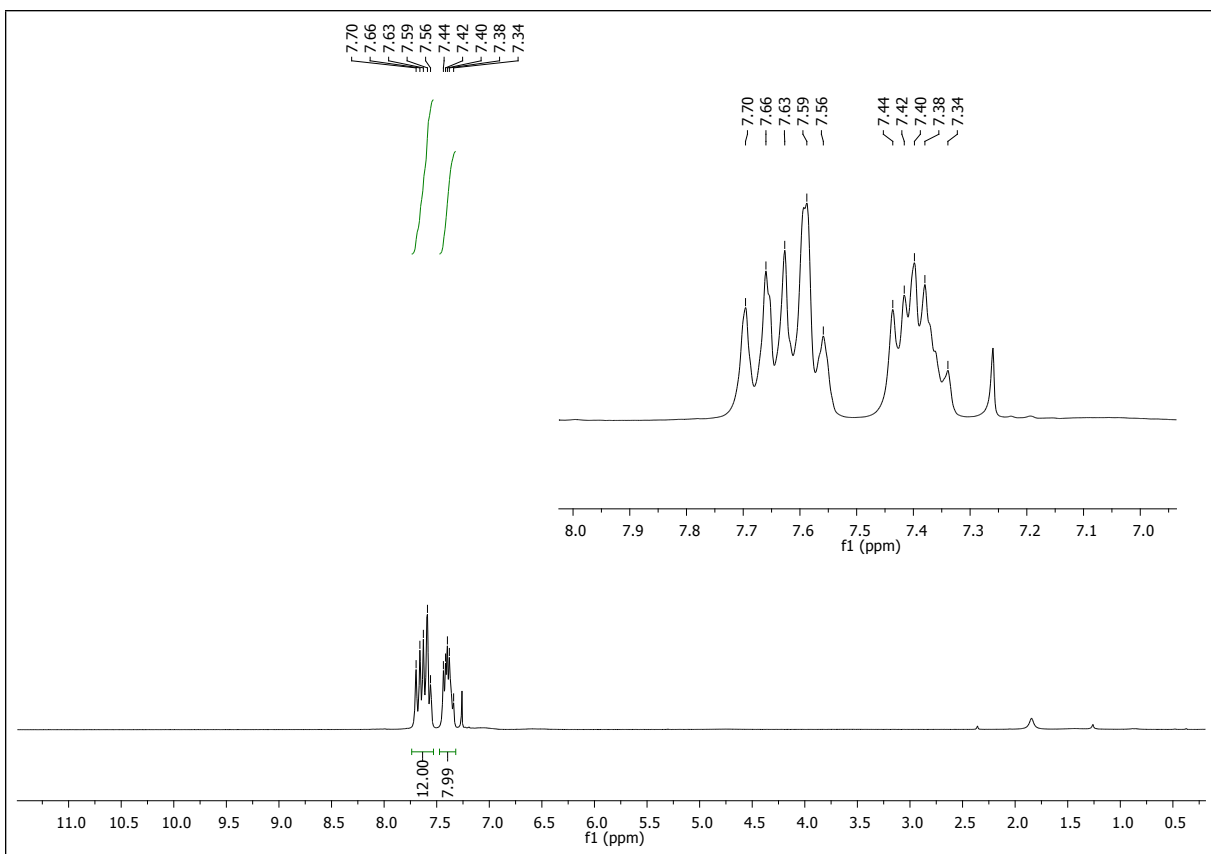


Figure S15. ^1H -NMR of **3** (CDCl_3).

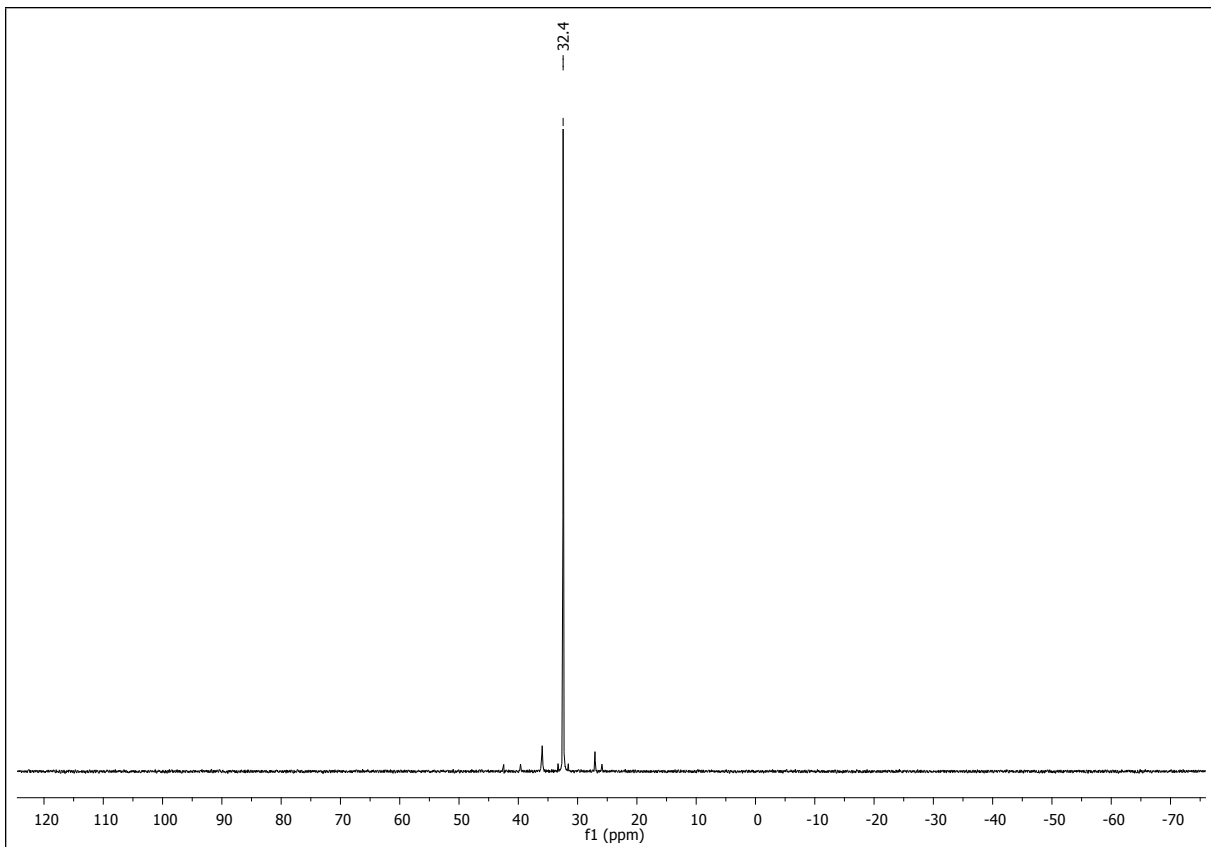


Figure S16. $^{31}\text{P}\{^1\text{H}\}$ -NMR of **4** ($\text{THF-}d_8$).

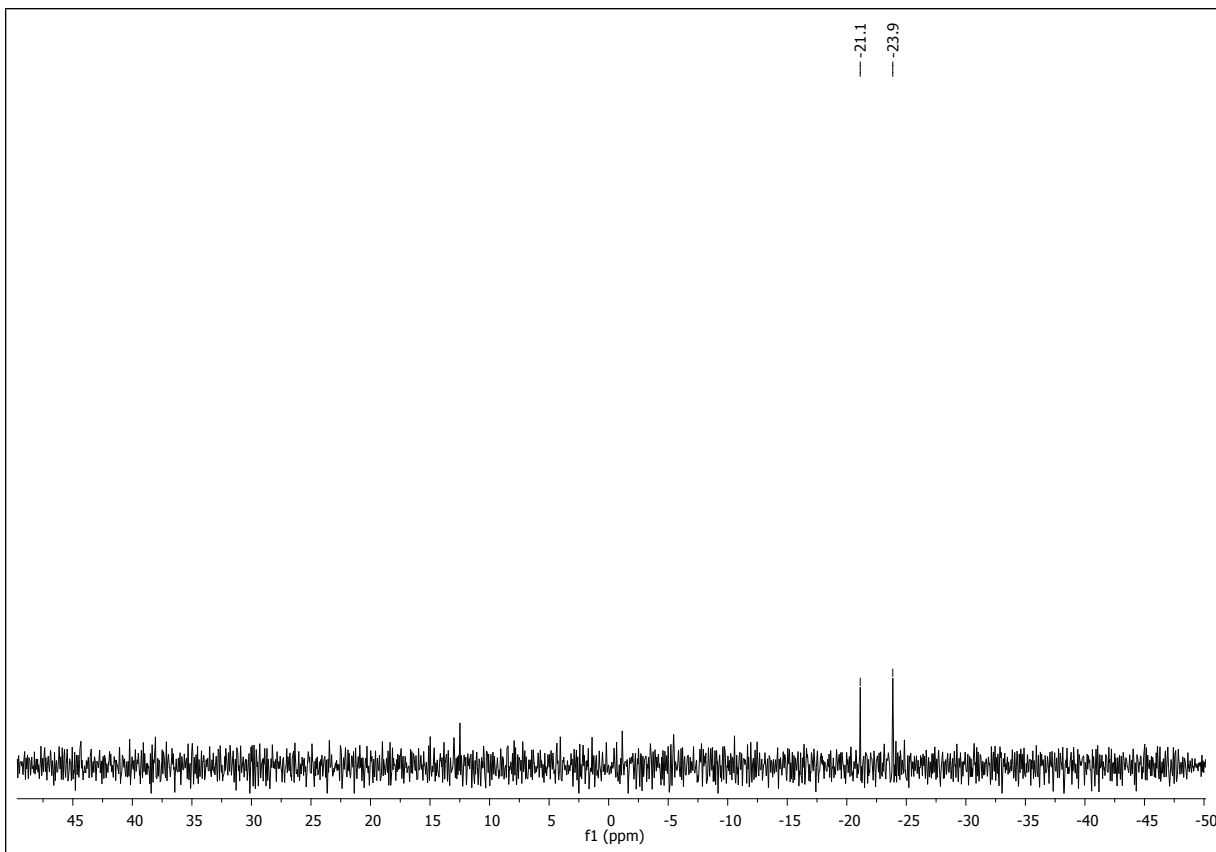


Figure S17. $^{29}\text{Si}\{\text{H}\}$ -NMR of **4** ($\text{THF}-d_8$).

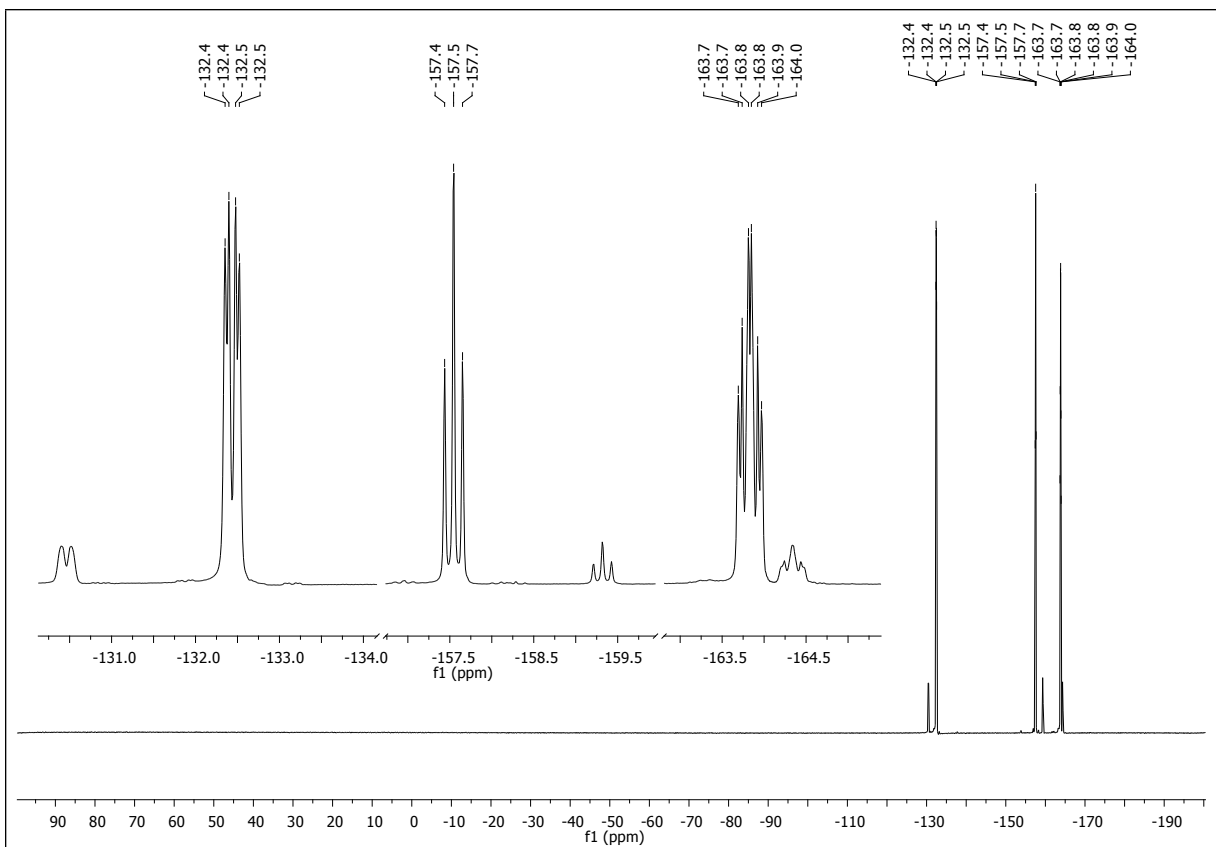


Figure S18. $^{19}\text{F}\{\text{H}\}$ -NMR of **4** ($\text{THF}-d_8$).

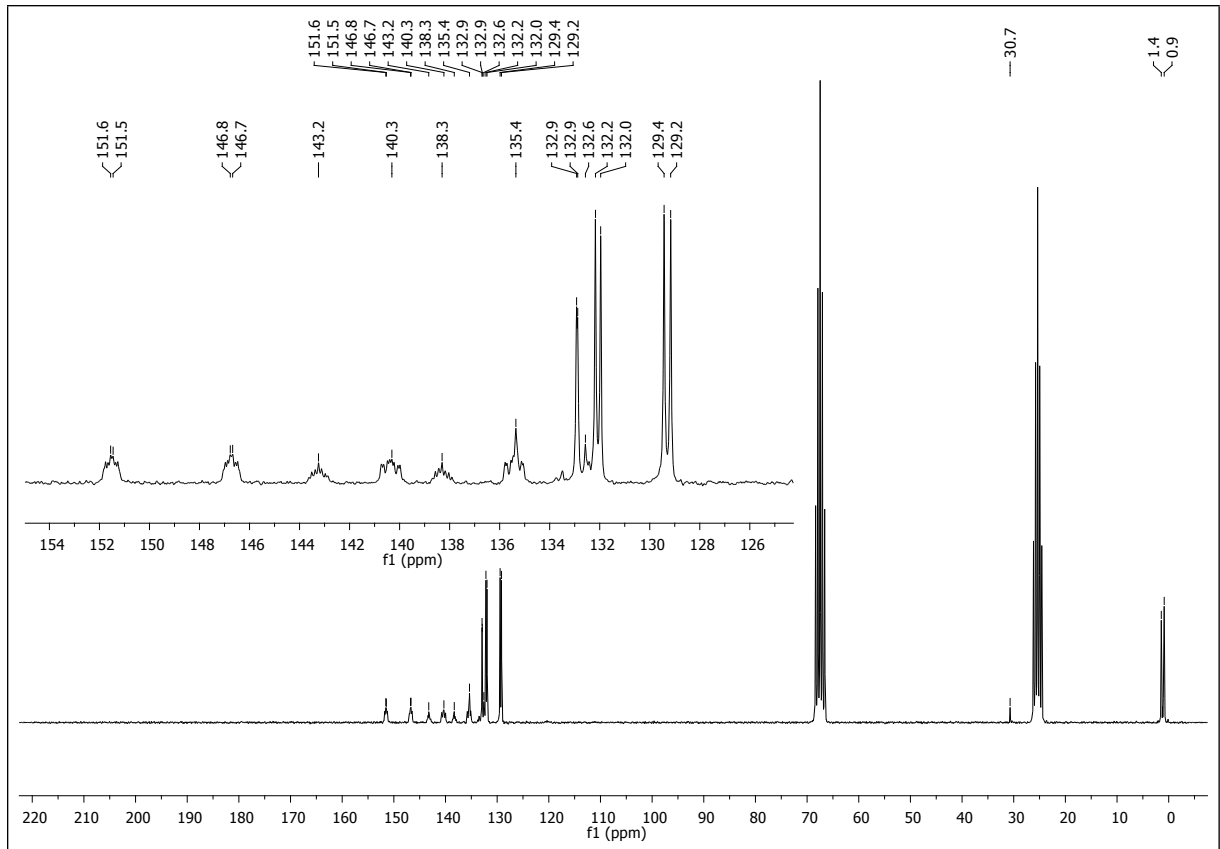


Figure S19. $^{13}\text{C}\{\text{H}\}$ -NMR of **4** (THF-*d*₈).

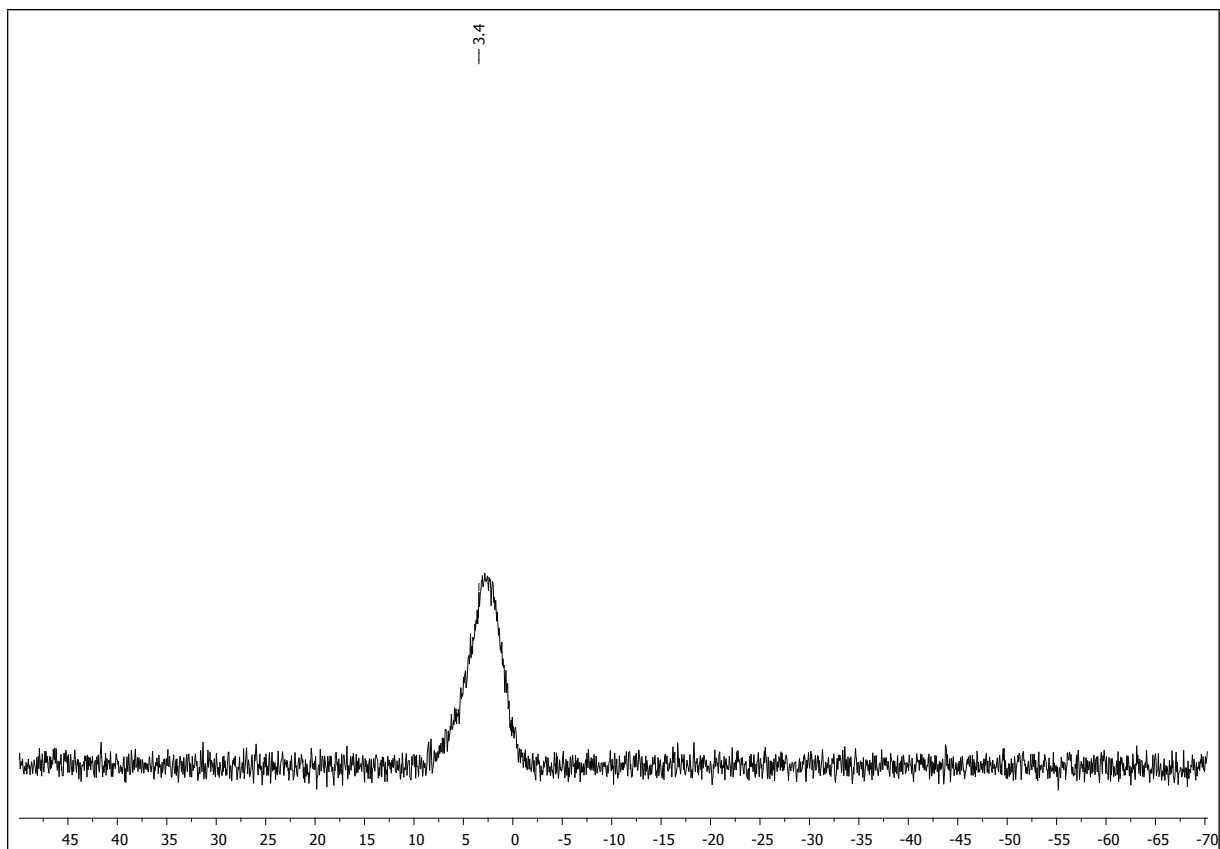


Figure S20. $^{11}\text{B}\{^1\text{H}\}$ -NMR of **4** (THF- d_8).

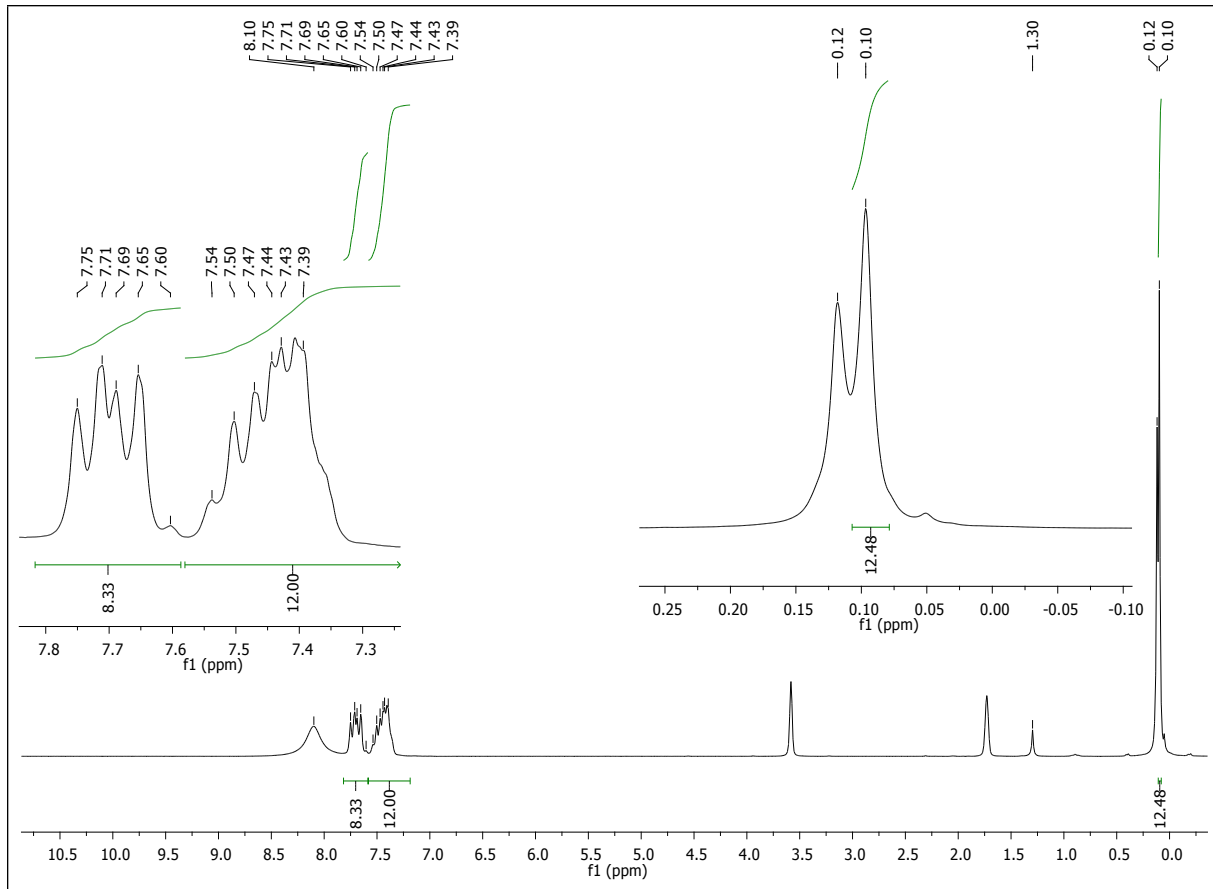


Figure S21. ^1H -NMR of **4** (THF- d_8).

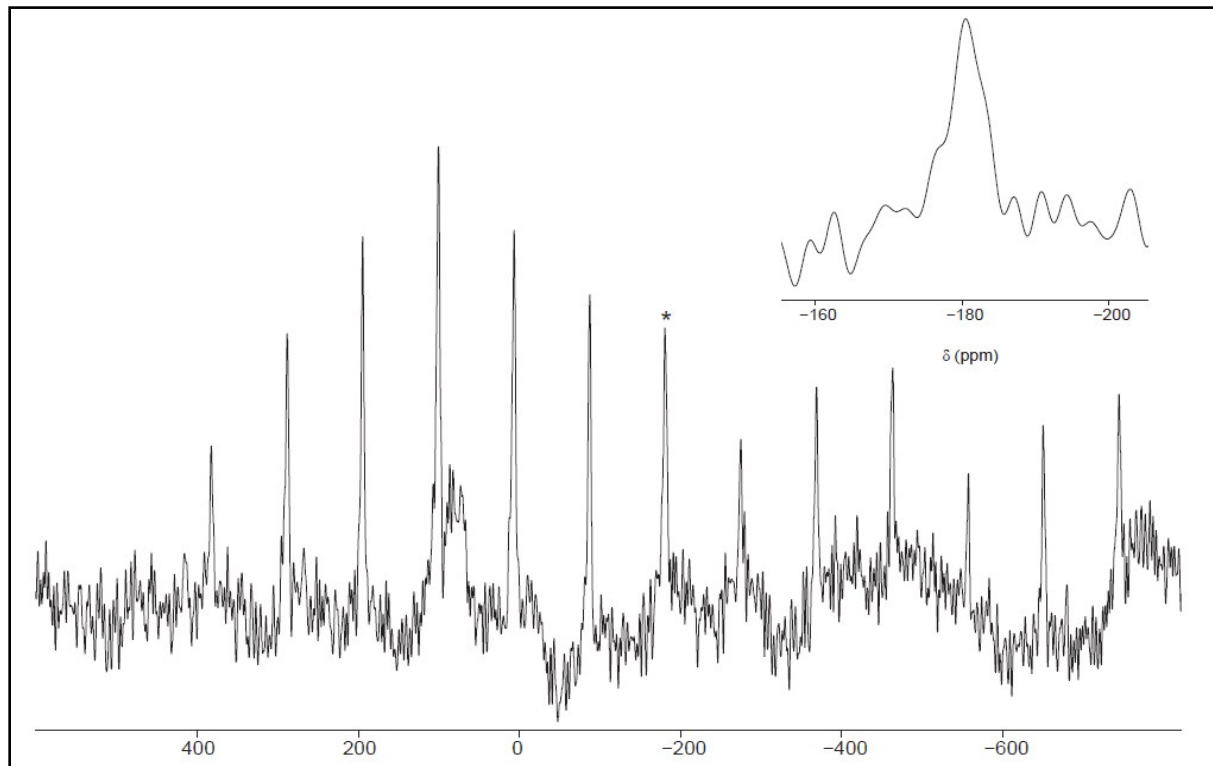


Figure S22. Solid state ^{119}Sn -NMR spectrum of **5** (isotropic chemical shift is marked with a star).

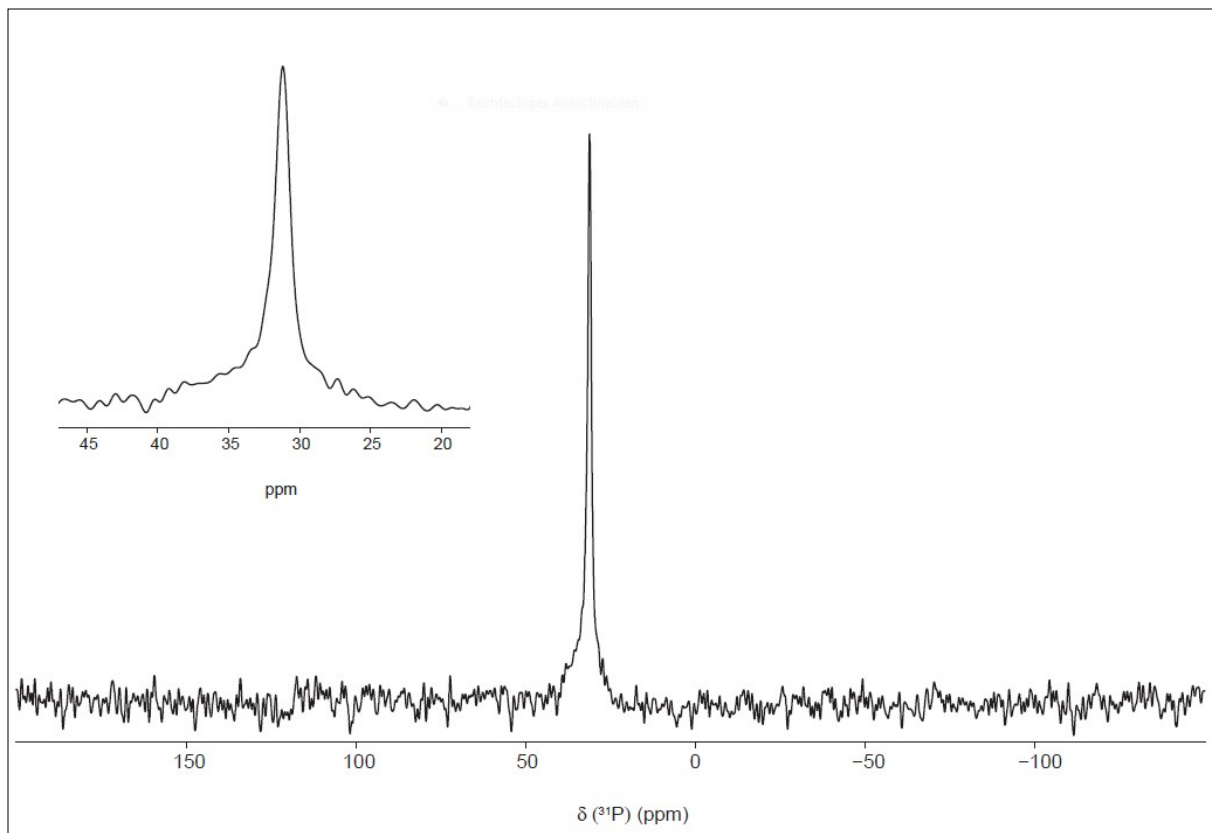


Figure S23. Solid state ^{31}P -NMR spectrum of **5**.

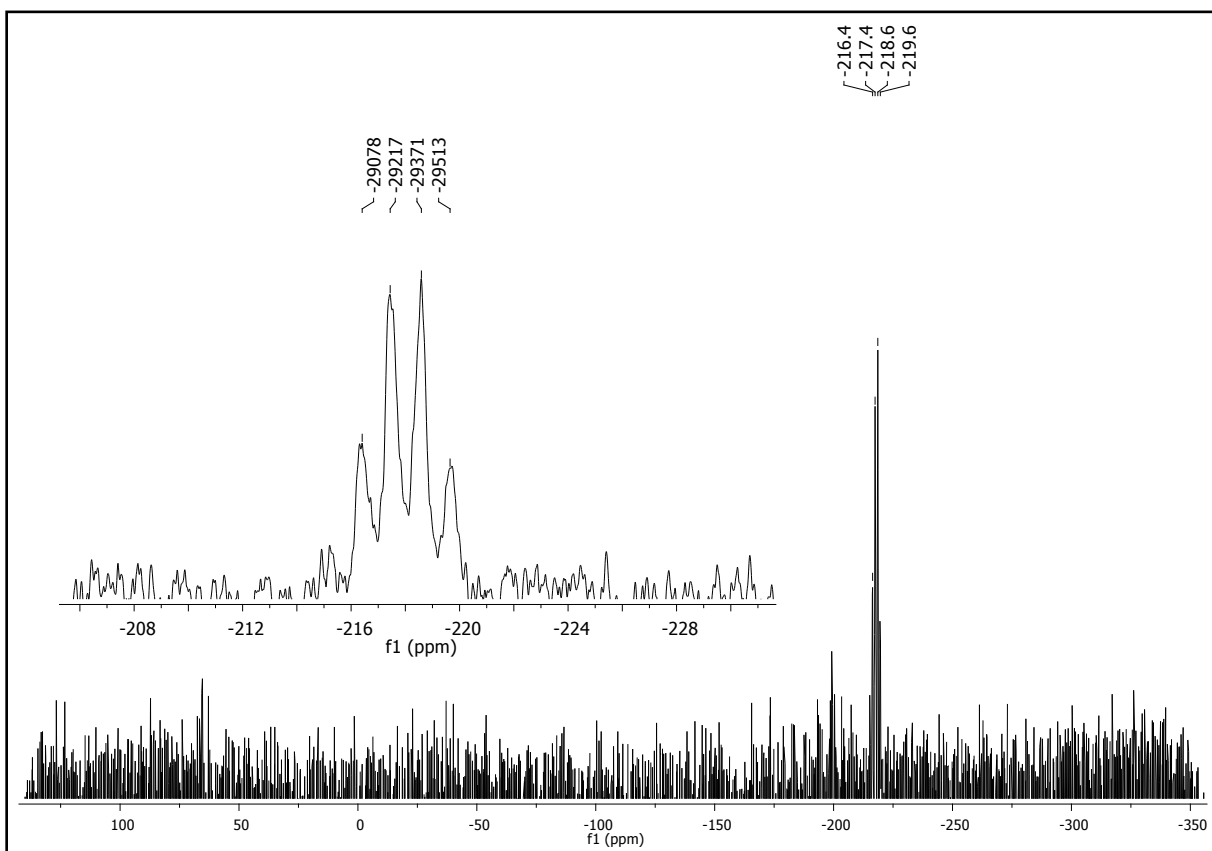
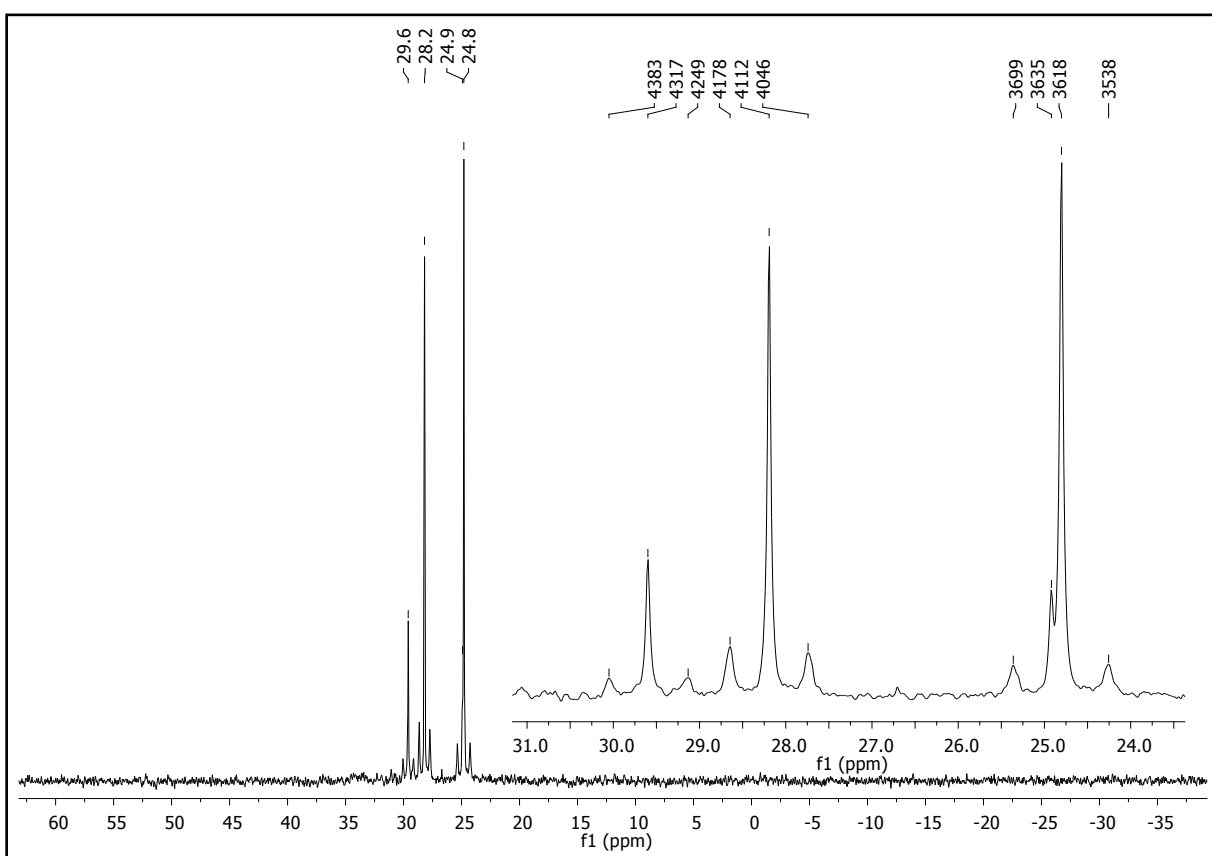
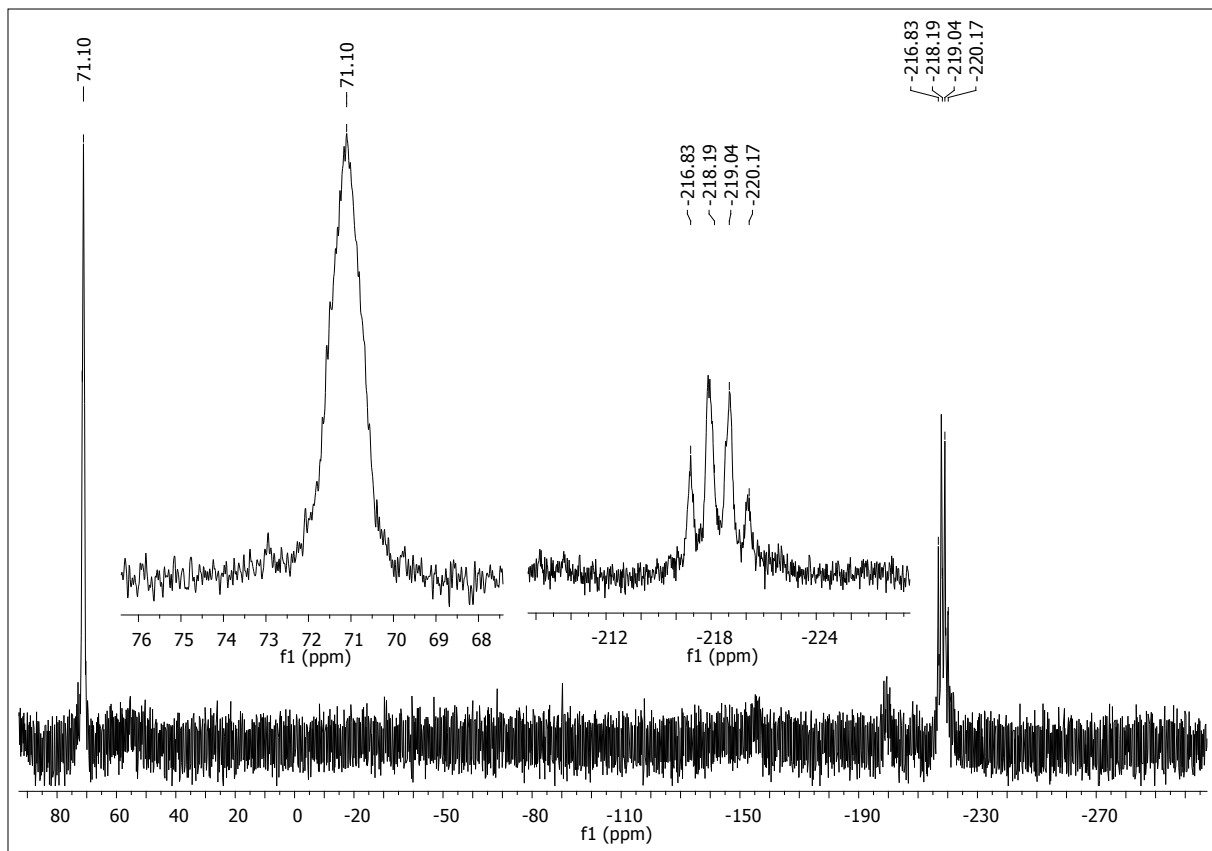


Figure S24. $^{119}\text{Sn}\{^1\text{H}\}$ -NMR of **5** (C_6D_6).



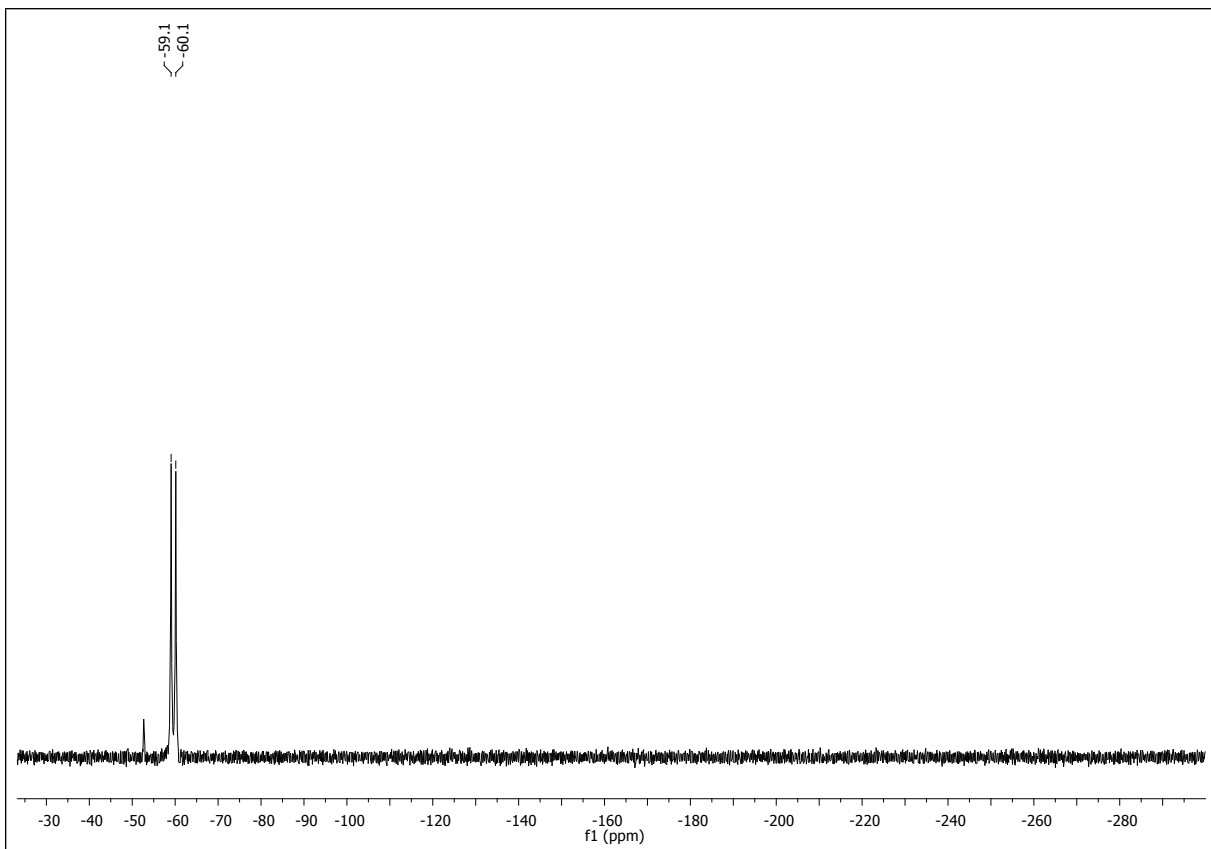


Figure S27. $^{119}\text{Sn}\{^1\text{H}\}$ -NMR of **6** (CDCl_3).

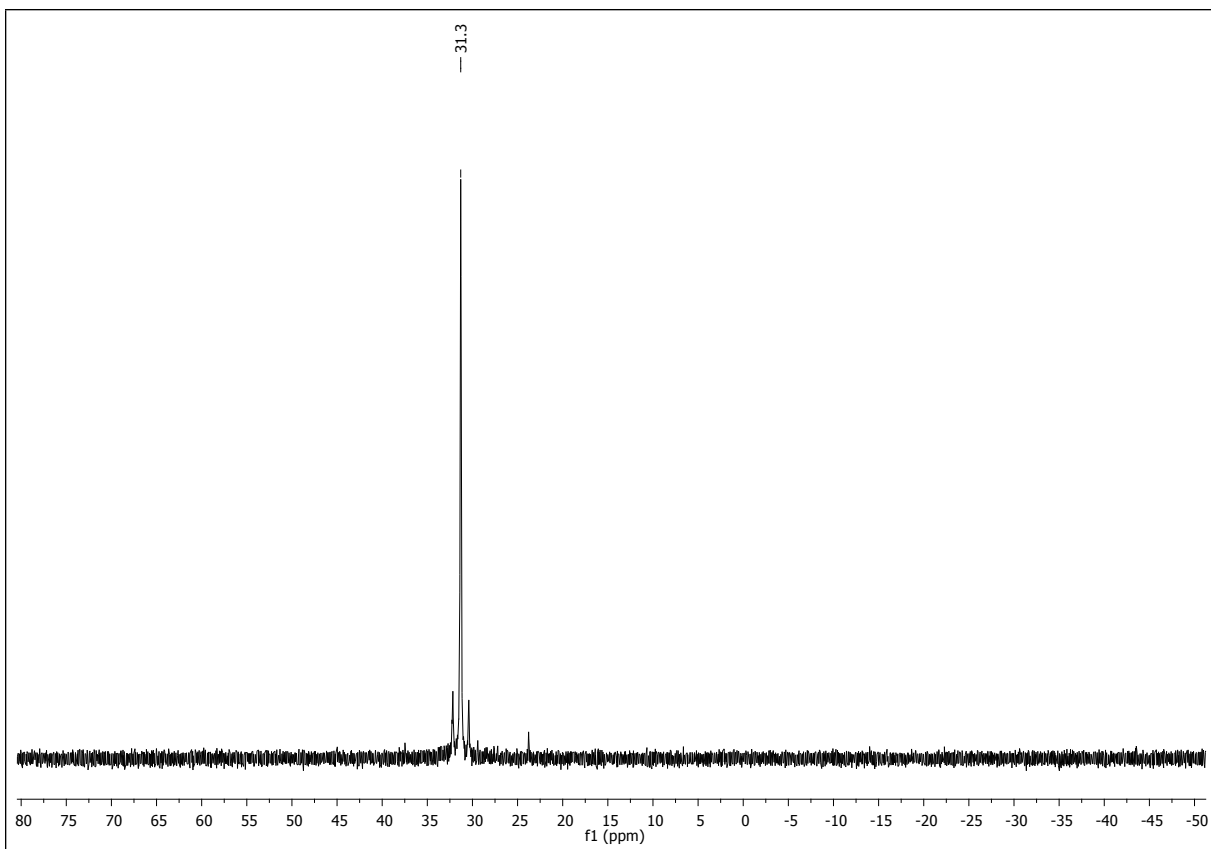


Figure S28. $^{31}\text{P}\{^1\text{H}\}$ -NMR of **6** (CDCl_3)

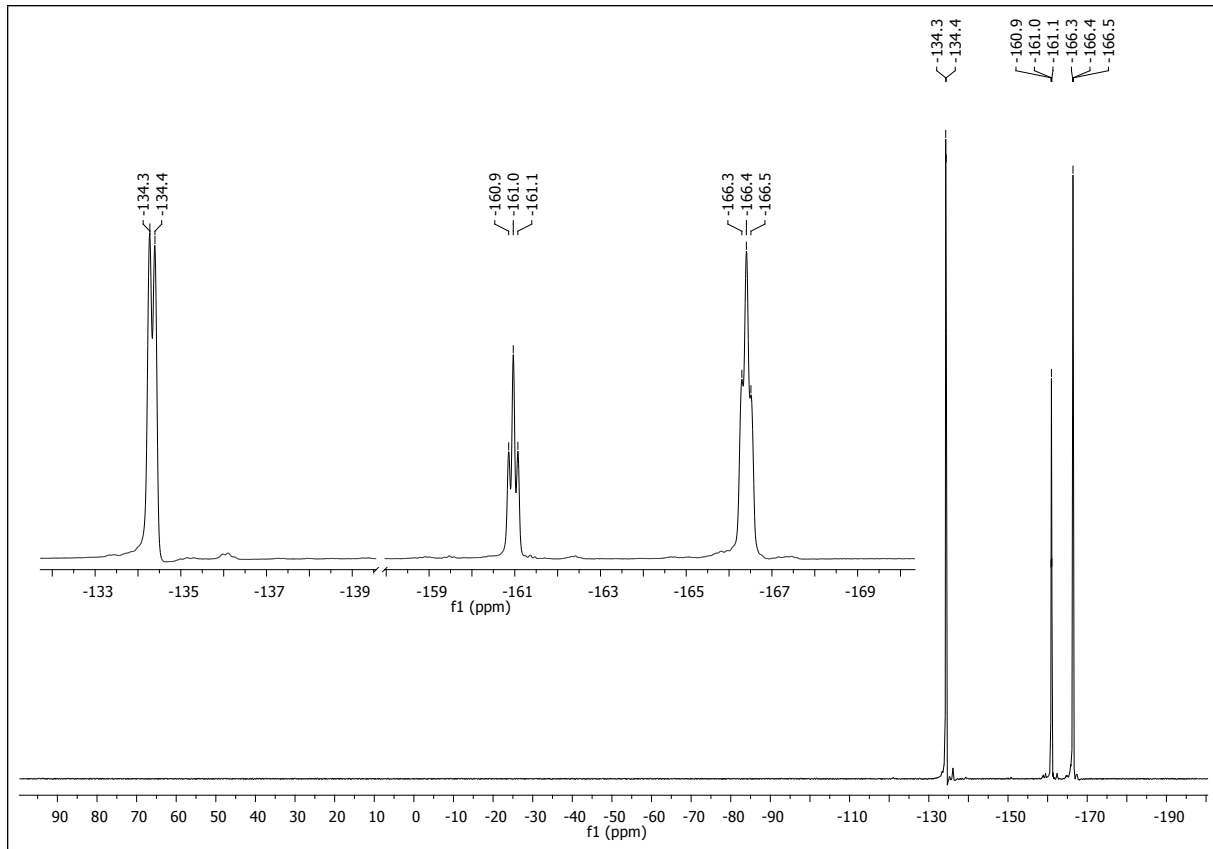


Figure S29. $^{19}\text{F}\{^1\text{H}\}$ -NMR of **6** (CDCl_3).

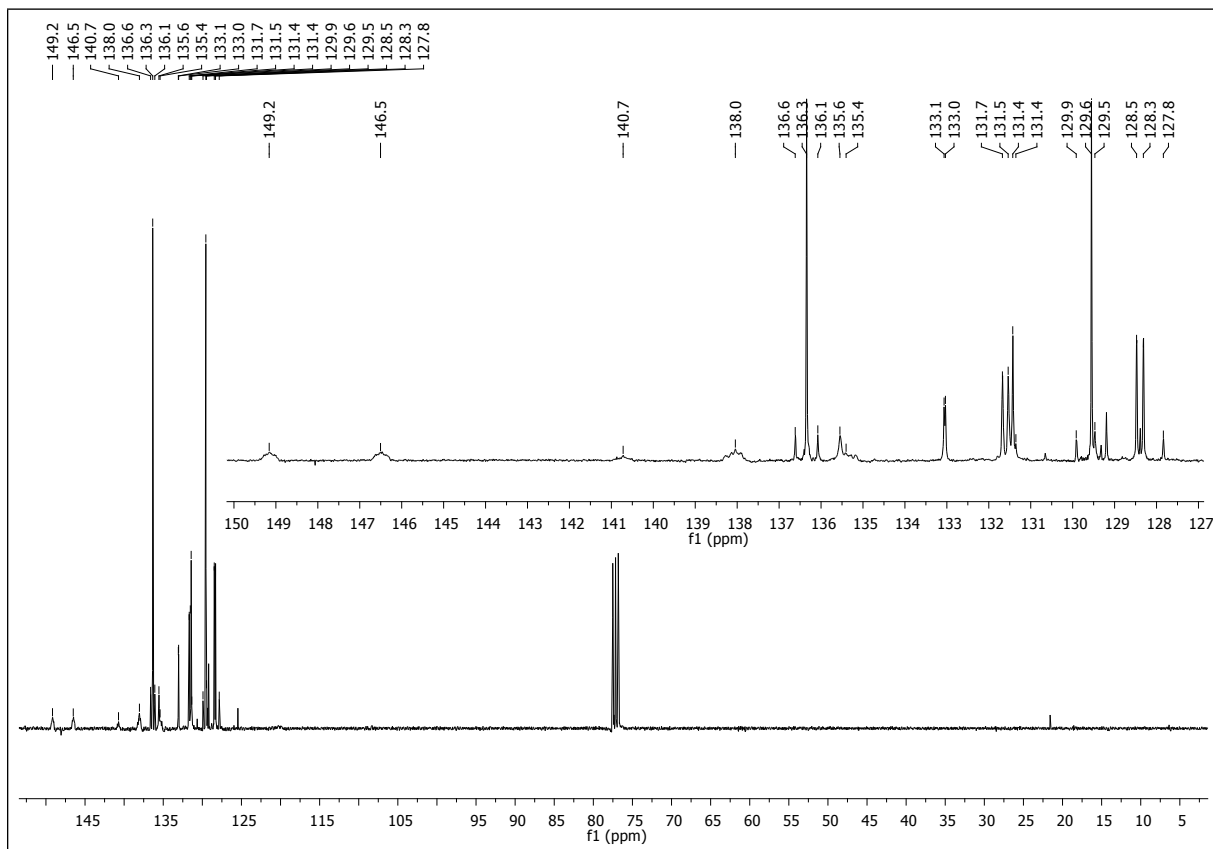


Figure S30. $^{13}\text{C}\{\text{H}\}$ -NMR of **6** (CDCl_3).

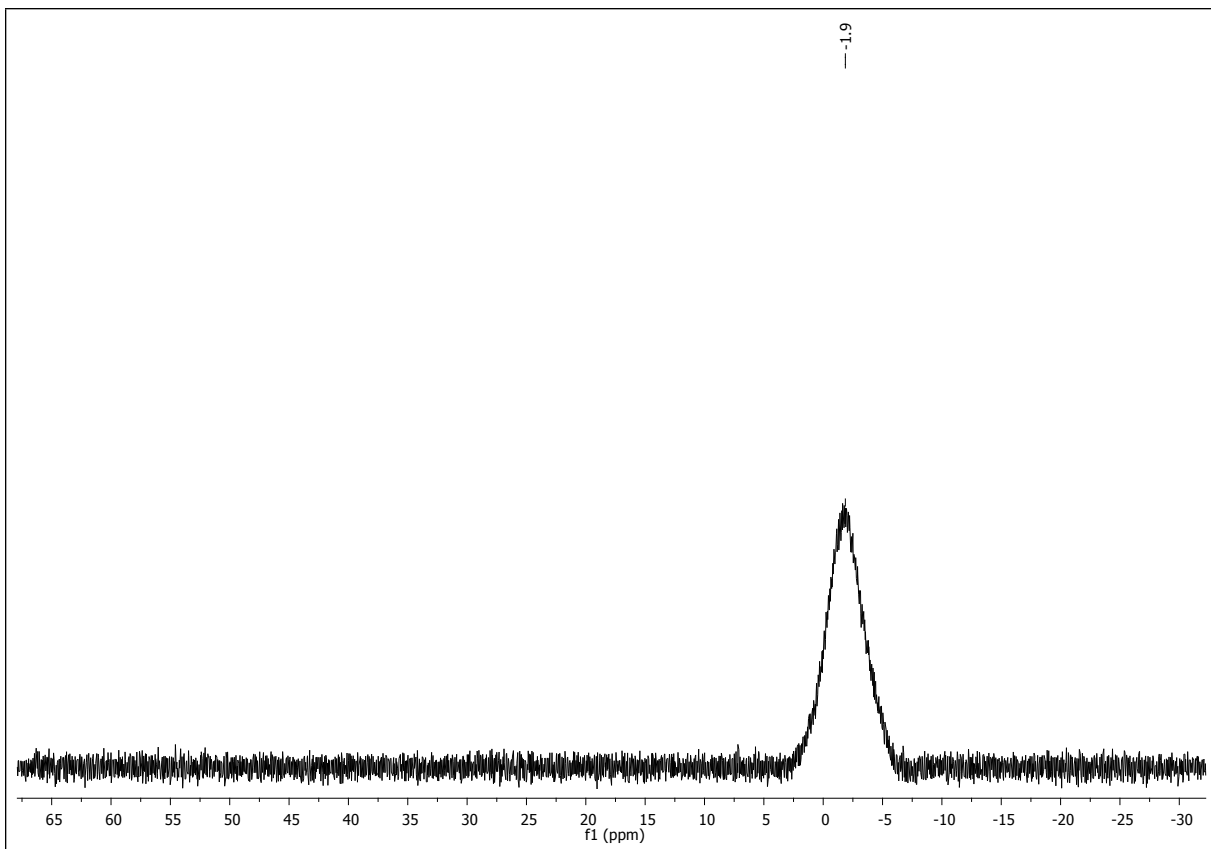


Figure S31. $^{11}\text{B}\{^1\text{H}\}$ -NMR of **6** (CDCl_3).

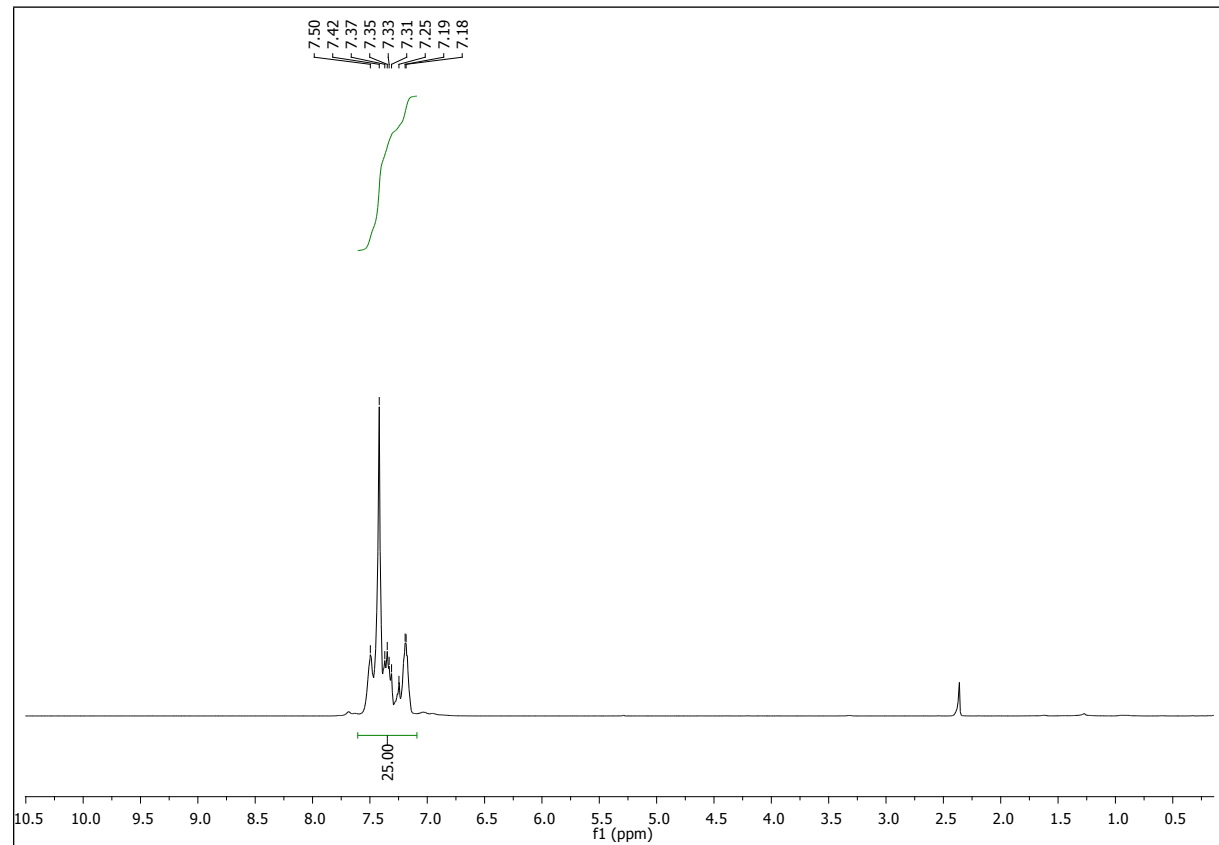


Figure S32. ^1H -NMR of **6** (CDCl_3).

X-ray crystallography. Intensity data were collected on Bruker Venture D8 diffractometer (**2**, **5**, **6**) at 100K, a Siemens P4 diffractometer (**3**) at 173 K and STOE IPDS 2T imaging plate (**4**) at 173 K with graphite-monochromated Mo-K α (0.7107 Å) radiation. All structures were solved by direct methods and refined based on F² by use of the SHELX program package as implemented in WinGX.^[S3] All non-hydrogen atoms were refined using anisotropic displacement parameters. Hydrogen atoms attached to carbon atoms were included in geometrically calculated positions using a riding model. Hydrogen atoms attached to oxygen atoms were located during in the electron density map and refined isotropically. Disorder was resolved for O5-O7 and C64-C67 of **2** and refined with split occupancies of 50:50 over two positions. Crystal and refinement data are collected in Table S1. Figures were created using DIAMOND.^[S4] Crystallographic data (excluding structure factors) for the structural analyses have been deposited with the Cambridge Crystallographic Data Centre, CCDC nos. 1411098 - 1411113. Copies of this information may be obtained free of charge from The Director, CCDC, 12 Union Road, Cambridge CB2 1EZ, UK (Fax: +44-1223-336033; e-mail: deposit@ccdc.cam.ac.uk or <http://www.ccdc.cam.ac.uk>)

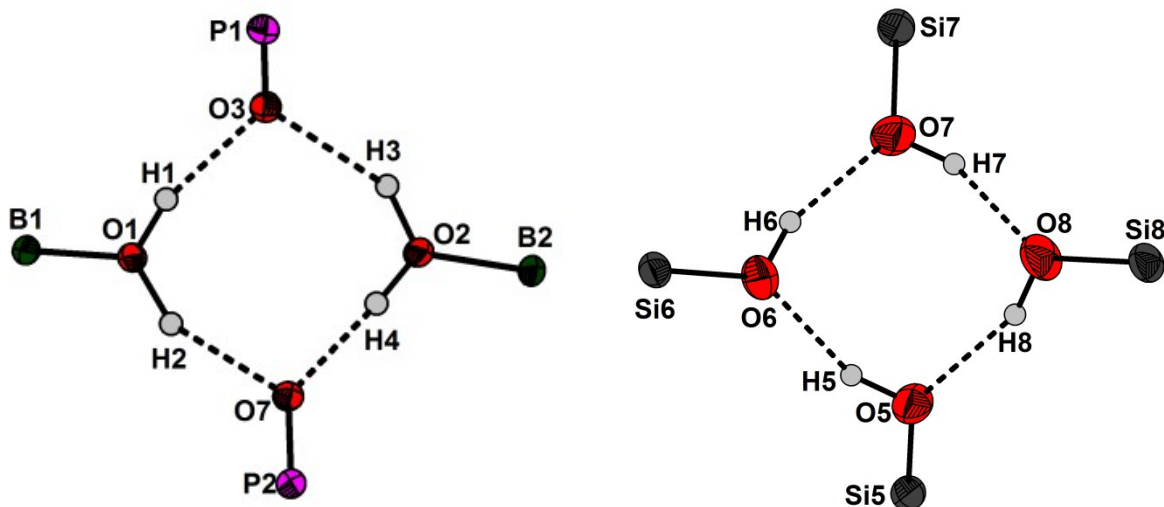


Figure S33. Hydrogen bond motifs of **4** and Ph₃SiOH (redrawn from the literature ^[14]) comprising the binary graph set R₄(8).

Table S1. Crystal data and structure refinement of **2 - 6**.

	2	3
Formula	C ₄₀ H ₂₆ BF ₁₅ NaO ₇ P	C ₄₈ H ₂₀ B ₂ F ₂₀ O ₄ P ₂
Formula weight, g mol ⁻¹	968.38	1124.20
Crystal system	monoclinic	orthorhombic
Crystal size, mm	0.2 × 0.1 × 0.1	0.8 × 0.7 × 0.5
Space group	P2 ₁ /c	P2 ₁ 2 ₁ 2 ₁
<i>a</i> , Å	10.0891(6)	13.371(2)
<i>b</i> , Å	18.980(1)	17.403(4)
<i>c</i> , Å	20.874(1)	19.327(4)
α , °	90	90
β , °	93.041(2)	90
γ , °	90	90
<i>V</i> , Å ³	3991.6(4)	4497(2)
<i>Z</i>	4	4
ρ_{calcd} , Mg m ⁻³	1.611	1.660
μ (Mo $K\alpha$), mm ⁻¹	0.201	0.227
<i>F</i> (000)	1952	2240
θ range, deg	2.29 to 27.05	2.57 to 27.50
Index ranges	$-12 \leq h \leq 12$ $-24 \leq k \leq 24$ $-26 \leq l \leq 26$	$-17 \leq h \leq 15$ $-22 \leq k \leq 12$ $-25 \leq l \leq 25$
No. of reflns collected	150205	12868
Completeness to θ_{max}	99.9%	99.8%
No. indep. Reflns	8745	9606
No. obsd reflns with ($I > 2\sigma(I)$)	6794	8369
No. refined params	649	685
GooF (F^2)	1.058	1.021
$R_1(F)$ ($I > 2\sigma(I)$)	0.0437	0.0374
$wR_2(F^2)$ (all data)	0.1145	0.0912
Largest diff peak/hole, e Å ⁻³	0.692 / -0.388	0.226 / -0.238
CCDC number	1480495	1480498

Table S1. cont.

4	5	6
C ₆₄ H ₃₆ B ₂ F ₃₀ O ₇ P ₂ Si ₂	C ₆₄ H ₃₄ B ₂ F ₃₀ O ₆ P ₂ Sn ₂	C ₄₈ H ₂₅ BF ₁₅ O ₂ PSn
1626.67	1789.85	1079.15
monoclinic	monoclinic	monoclinic
0.5 × 0.4 × 0.1	0.09 × 0.045 × 0.04	0.1 × 0.08 × 0.05
P2 ₁ /c	C2/c	P2 ₁ /c
23.373(5)	19.3191(6)	12.5234(5)
12.322(3)	19.1291(6)	29.972(1)
23.430(5)	23.6401(8)	12.5099(5)
90	90	90
91.95(3)	109.260(1)	116.242(1)
90	90	90
6744(2)	8247.4(5)	4211.6(3)
4	4	4
1.602	1.441	1.702
0.236	0.754	0.753
3256	3504	2136
2.40 to 26.16	2.62 to 27.50	2.27 to 30.11
-28 ≤ h ≤ 28	-24 ≤ h ≤ 24	-17 ≤ h ≤ 17
-14 ≤ k ≤ 14	-24 ≤ k ≤ 24	-42 ≤ k ≤ 42
-28 ≤ l ≤ 28	-30 ≤ l ≤ 30	-17 ≤ l ≤ 17
46041	112132	158063
98.5%	99.9%	99.8%
12869	9045	12390
5696	7641	10589
984	482	613
1.061	1.088	1.048
0.0561	0.0355	0.0293
0.1367	0.0904	0.0662
0.242 / -0.459	0.706 / -0.558	0.577 / -0.429
1480497	1480496	1480499

X-ray powder diffraction. Intensity data was collected on a StadiP diffractometer (Stoe and Cie GmbH, Darmstadt, Germany) in a fused glass capillary (outer diameter $d = 0.3$ mm) in Debye-Scherrer-geometry. The instrument is equipped with a Ge(111)-monochromator and a linear PSD detector. The data was collected in a range of $3 - 60^\circ 2\theta$, ($\text{CuK}_{\alpha 1}$) with a step size of $0.01^\circ 2\theta$. Rietveld refinements and Pawley-fits were carried out using DiffracPlus Topas 4.2^[S5] and the fundamental parameter approach for the refinements. The fundamental parameter set was obtained by fitting instrumental parameters against a LaB_6 standard reference material and have been verified by Si standard reference material. The Pawley-fit (Figure S33) shows that the unit cell determined in the single crystal diffraction is able to describe well the full powder diffraction data and converges with a R_{wp} value of 3.20 %. The lattice parameters were refined to be $a = 1995.3(1)$ pm, $b = 1952.6(1)$ pm and $c = 2388.9(1)$ pm. The monoclinic angle was calculated to be $\beta = 109.755(3)^\circ$.

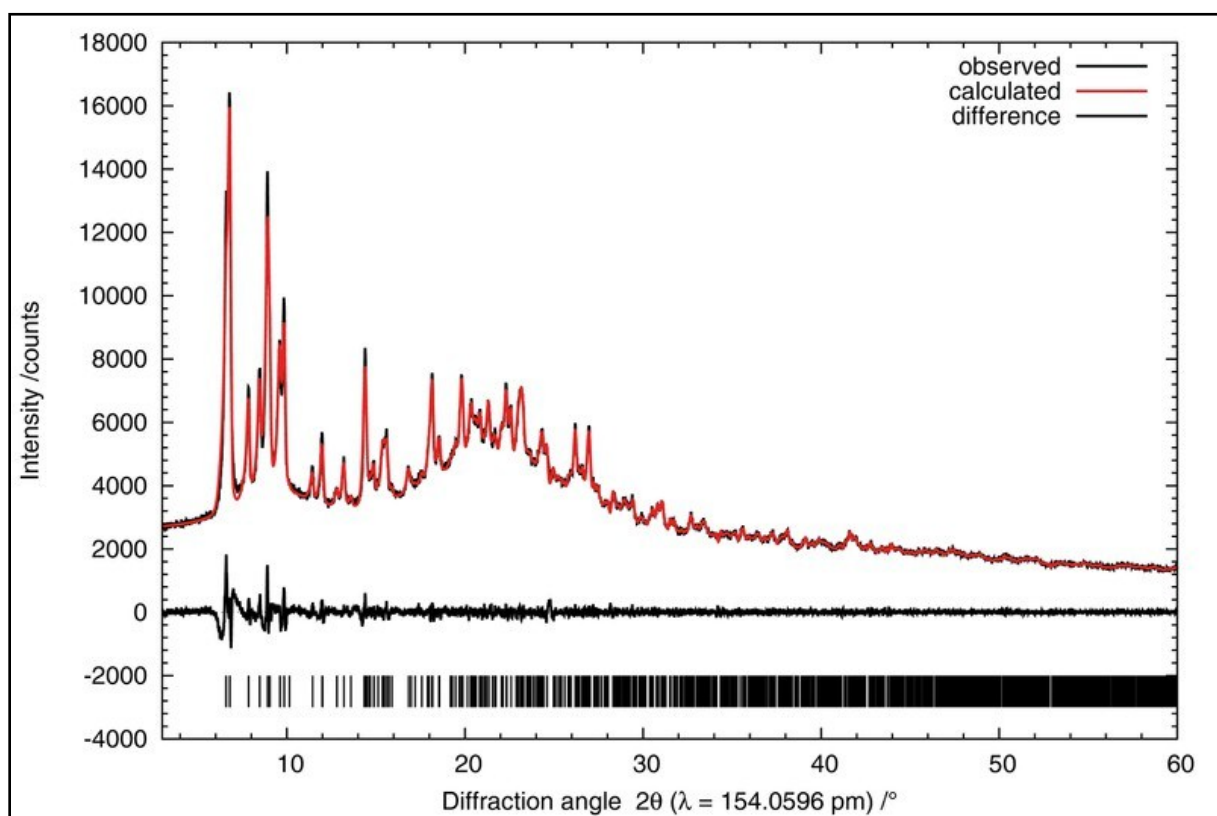
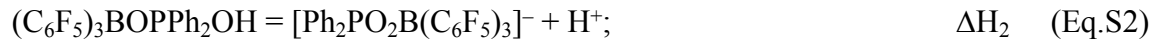


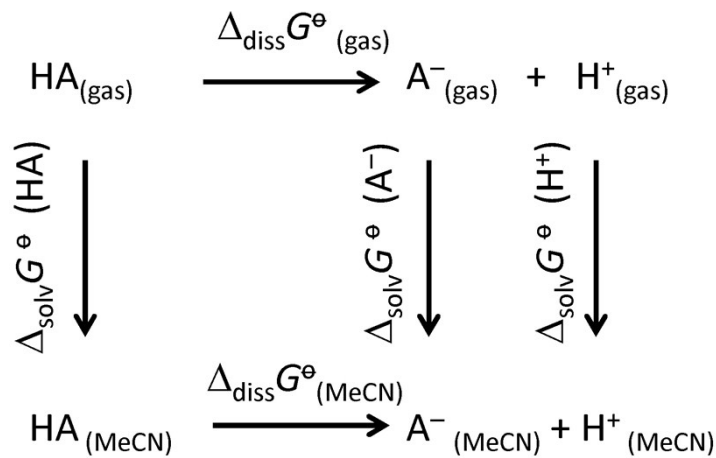
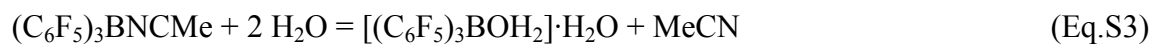
Figure S34. Powder diffraction of **6** (Pawley-fit).

Computational details. To analyze the electronic structures of the acids and conjugate bases the gas-phase molecular geometries of Ph₂PO₂H, [Ph₂PO₂]⁻, (C₆F₅)₃BOPPh₂OH (**1**) and [Ph₂PO₂B(C₆F₅)₃]⁻ (anion of **2**) were optimized using the Gaussian09 program suit^[S6] at the M062X/DGDZVP level of theory employed earlier for calculations of the donor acceptor complexes Ph₃EOB(C₆F₅)₃ (E = P, As, Sb).^[S7] The calculated and experimental bond lengths are compared in Table S2. The optimization procedure was accompanied by the frequency calculations to confirm the energy minima corresponding to the final structures. The QTAIM theory^[S8] was used to calculate the atomic charges (Table S3) with the AIMALL package.^[S9] The deformation electron density (DED) maps (Figures S34, S35) were built with the Multiwfn program^[S10] by subtracting the electron densities of individual sphericalized atoms from the total molecular electron density. The pK_{a(MeCN)} values were calculated using the SMD continuum solvation model.^[S11] We chose the M052X/6-31+G** level of theory listed among those taken for the optimization of the SMD parameters.^[S11] DFT calculations were performed for Ph₂PO₂H, (C₆F₅)₃BOPPh₂OH and (C₆F₅)₃BOH₂ as well as for 15 tabulated^[S12] acids and the corresponding conjugate bases (Tables S4, S5). The acid and conjugate base structures were optimized and the vibrational frequencies were computed in the gas phase and MeCN solution with the Gaussian 09 package.^[S6] The sums of electronic and thermal Gibbs free energies were used initially to calculate the $\Delta_{\text{diss}}G^{\ominus}$ (gas) values for the gas-phase acid dissociations at 298.15 K (Scheme S1). The proton gas-phase free energy was taken as -6.28 kcal mol⁻¹.^[S13] The pK_{a(gas)} values were then determined as pK_{a(gas)} = $\Delta_{\text{diss}}G^{\ominus}$ (gas)/2.303RT (Table S4). The $\Delta_{\text{solv}}G^{\ominus}$ (HA) and $\Delta_{\text{solv}}G^{\ominus}$ (A⁻) parameters were defined as the differences between the SCF energies in MeCN as recommended earlier.^[S14] The $\Delta_{\text{solv}}G^{\ominus}$ (A⁻) = -251.9 kcal mol⁻¹ proton solvation free energy was used.^[S14] On the basis of these data the $\Delta_{\text{diss}}G^{\ominus}_{(\text{MeCN})}$ values (Scheme S1) were calculated taking in to account the 1.9 kcal mol⁻¹ correction^[S13] for the standard state change on going from the gas (the pressure of 1 bar) to solution phase (the concentration of 1 mol L⁻¹). The theoretical pKa values correlate well with the experimental data (Tables S4 and S5). The pK_{a,calc} - pK_{a,exp} differences can be explained by the dissociation model (Scheme S1) which neglects the homoassociation reactions between the ions and the conjugate acids.^[S12b] To increase the reliability of our theoretical predictions the experimental pK_{a,exp} values were plotted against calculated pK_{a,calc} (Figures S37 and S38). Then the expected pKa magnitudes were determined on the basis of linear regression analysis (Tables S4 and S5). The mean absolute error (MAE) determined from the differences between the experimental and predicted pKa values decreases from 3.5 to 1.9 on going from pK_{a,calc} (gas) to pK_{a,cor (gas)} and from 1.6 to 1.0 on going from pK_{a,calc (MeCN)} to pK_{a,cor (MeCN)}.

The M052X/6-31+G** level of theory was also used to estimate the difference in the Ph₂PO₂H and **1** dissociation enthalpies (Eqs. S1 and S2) $\Delta\Delta H = \Delta H_1 - \Delta H_2$.



The $\Delta\Delta H$ was found as a difference between the sums of electronic energies in MeCN solution: $\Delta\Delta H = \{E_{\text{el}}([\text{Ph}_2\text{PO}_2]^-) + E_{\text{el}}((\text{C}_6\text{F}_5)_3\text{BOPPh}_2\text{OH})\} - \{E_{\text{el}}(\text{Ph}_2\text{PO}_2\text{H}) + E_{\text{el}}([\text{Ph}_2\text{PO}_2\text{B}(\text{C}_6\text{F}_5)_3]^-)\}$. The enthalpy of the reaction between ($\text{C}_6\text{F}_5)_3\text{BNCMe}$ and H_2O (Eq. S3) in MeCN solution calculated at the M052X/6-31+G** level on the basis of the reactant and product electronic energies ($-9.0 \text{ kcal mol}^{-1}$) appears to be very close to the experimental^[S12b] value of $-8.6 \text{ kcal mol}^{-1}$.



Scheme S1. Thermodynamic circle used for the pKa calculations

Table S2. Calculated at the M062X/DGDZVP, M052X/6-31+G** levels of theory (gas phase) and experimental^[22, S15-S17] (X-ray crystal structures) selected interatomic distances (\AA) in the representative acids and conjugate bases studied.

Bond	1	anion of 2	Ph ₂ PO ₂ H	[Ph ₂ PO ₂] ⁻	(C ₆ F ₅) ₃ BOH ₂	[(C ₆ F ₅) ₃ BOH] ⁻
B-O1 (M062X/DGDZVP)	1.546	1.503	-	-	-	-
B-O1 (M052X/6-31+G**)	1.549	1.506	-	-	1.656	1.460
B-O1 (experiment)	-	1.508 ^b	-	-	1.630 ^e	1.466 ^f
P-O1 (M062X/DGDZVP)	1.528	1.575	1.484	1.506	-	-
P-O1 (M052X/6-31+G**)	1.530	1.577	1.489	1.513	-	-
P-O1 (experiment)	-	1.544 ^b	1.501 ^c	1.508 ^d	-	-
P-O2 (M062X/DGDZVP)	1.595	1.489	1.626	1.506	-	-
P-O2 (M052X/6-31+G**)	1.599	1.495	1.632	1.513	-	-
P-O2 (experiment)	-	1.482 ^b	1.550 ^c	1.508 ^d	-	-
B-C (M062X/DGDZVP)	1.632 ^a	1.650 ^a	-	-	-	-
B-C (M052X/6-31+G**)	1.635 ^a	1.652 ^a	-	-	1.619 ^a	1.664 ^a
B-C (experiment)	-	1.651 ^a	-	-	1.627 ^{a, e}	1.663 ^{a, f}
P-C (M062X/DGDZVP)	1.786 ^a	1.817 ^a	1.804 ^a	1.852 ^a	-	-
P-C (M052X/6-31+G**)	1.789 ^a	1.820 ^a	1.806 ^a	1.851 ^a	-	-
P-C (experiment)	-	1.802 ^a	1.795 ^{a, c}	1.804 ^{a, d}	-	-

^a Averaged value. ^b This work. ^c Ref. S15. ^d Ref. S16. ^e Ref. 22. ^f Ref. S17.

Table S3. Mulliken (M062X/DGDZVP) / AIM atomic charges q on the O and H atoms of the OH groups in Ph₂PO₂H and (C₆F₅)₃BOPPh₂OH .

Molecule	q (O)	q (H)
Ph ₂ PO ₂ H	-0.80 / -1.34	+0.50 / +0.57
(C ₆ F ₅) ₃ BOPPh ₂ OH	-0.79 / -1.36	+0.55 / +0.62

Table S4. Experimental^[S12a] pKa_{exp}, calculated pKa_{calc} and expected on the basis of correlation analysis pKa_{cor} values for acids in the gas phase. The differences between the experimental and theoretical pKa_(gas) values are given.

Acid	pKa _{exp}	pKa _{calc}	pKa _{exp} – pKa _{calc}	pKa _{cor}	pKa _{exp} – pKa _{cor}
MeCO ₂ H	250.0	249.1	0.9	250.4	-0.4
PhCO ₂ H	244.1	242.8	1.3	244.6	-0.5
2,4,6-(NO ₂) ₃ C ₆ H ₃ OH	219.2	215.7	3.5	219.6	-0.4
2,4-(NO ₂) ₂ C ₆ H ₃ OH	226.2	226.9	-0.7	229.9	-3.7
(CN) ₃ CH	216.1	210.9	5.2	215.2	0.9
F ₃ CSO ₃ H	219.6	212.8	6.8	216.9	2.7
HCl	240.5	235.7	4.8	238.0	2.5
H ₃ PO ₄	236.8	233.1	3.7	235.6	1.2
Tf ₂ NH	210.0	207.8	2.2	212.3	-2.3
(C ₆ F ₅ SO ₂) ₂ NH	210.8	209.4	1.4	213.8	-3
(4-NO ₂ -C ₆ H ₄ SO ₂) ₂ NH	213.4	213.0	0.4	217.1	-3.7
2,4,6-(F ₃ CSO ₂) ₃ C ₆ H ₂ OH	213.9	206.6	7.3	211.2	2.7
(F ₃ CSO ₂) ₂ CHPh	219.9	214.6	5.3	218.6	1.3
FSO ₃ H	219.9	212.7	7.2	216.8	3.1
PhOH	250.9	249.8	1.1	251.0	-0.1
Ph ₂ PO ₂ H	-	237.0	-	239.2	-
(C ₆ F ₅) ₃ BOPPh ₂ OH	-	210.0	-	214.4	-
H ₂ O	281.3	282.4	-1.1	281.0	0.3
(C ₆ F ₅) ₃ BOH ₂	-	204.8	-	209.6	-

Table S5. Experimental^[S12b,S12c,3] pKa_{exp}, calculated pKa_{calc} and expected on the basis of correlation analysis pKa_{cor} values for acids in MeCN solution. The differences between the experimental and theoretical pKa_(MeCN) values are given.

Acid	pKa _{exp}	pKa _{calc}	pKa _{exp} – pKa _{calc}	pKa _{cor}	pKa _{exp} – pKa _{cor}
PhCO ₂ H	21.5	21.3	0.2	21.3	0.2
MeCO ₂ H	23.5	24.8	-1.3	24.5	-1
4-Me-C ₆ H ₄ SO ₃ H	8.5	8.1	0.4	9.6	-1.1
2,4,6-(NO ₂) ₃ C ₆ H ₃ OH	11	9.8	1.2	11.1	-0.1
HCl	8.5	5.8	2.7	7.5	1
4-CF ₃ -2,3,5-F ₄ C ₆ OH	16.6	13.8	2.8	14.7	1.9
4-NO ₂ C ₆ H ₄ SO ₃ H	6.7	5.4	1.3	7.2	-0.5
2,4-(NO ₂) ₂ C ₆ H ₃ OH	16.7	16.8	-0.1	17.3	-0.6
4-NO ₂ C ₆ H ₄ CH(CN) ₂	11.6	9.0	2.6	10.4	1.2
(F ₃ CSO ₂) ₂ NH	0.3	-1.7	2	0.9	-0.6
(F ₃ CSO ₂) ₃ C ₆ H ₂ OH	4.8	3.9	0.9	5.8	-1
(4-NO ₂ -C ₆ H ₄ SO ₂) ₂ NH	8.2	9.4	-1.2	10.7	-2.5
(F ₃ CSO ₂) ₂ CHPh	8.8	6.2	2.6	7.9	0.9
PhOH	29.1	29.0	0.1	28.2	0.9
F ₃ CSO ₃ H	0.7	-3.4	4.1	-0.6	1.3
Ph ₂ PO ₂ H	-	20.3	-	20.5	-
(C ₆ F ₅) ₃ BOPPh ₂ OH	-	7.9	-	9.4	-
H ₂ O	-	47.0	-	44.2	-
(C ₆ F ₅) ₃ BOH ₂	-	4.4	-	6.3	-

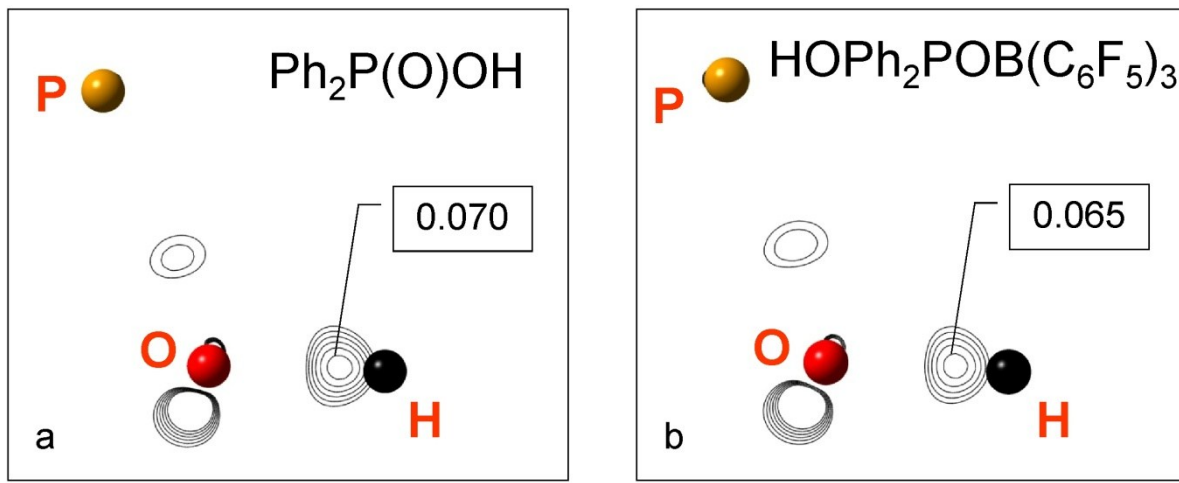


Figure S35. Profiles of the positive deformation electron density (0.045-0.070 a.u., step 0.005 a.u.) for $\text{Ph}_2\text{P}(\text{O})\text{OH}$ (a) and $(\text{C}_6\text{F}_5)_3\text{BOPPh}_2\text{OH}$ (b) in the POH plane.

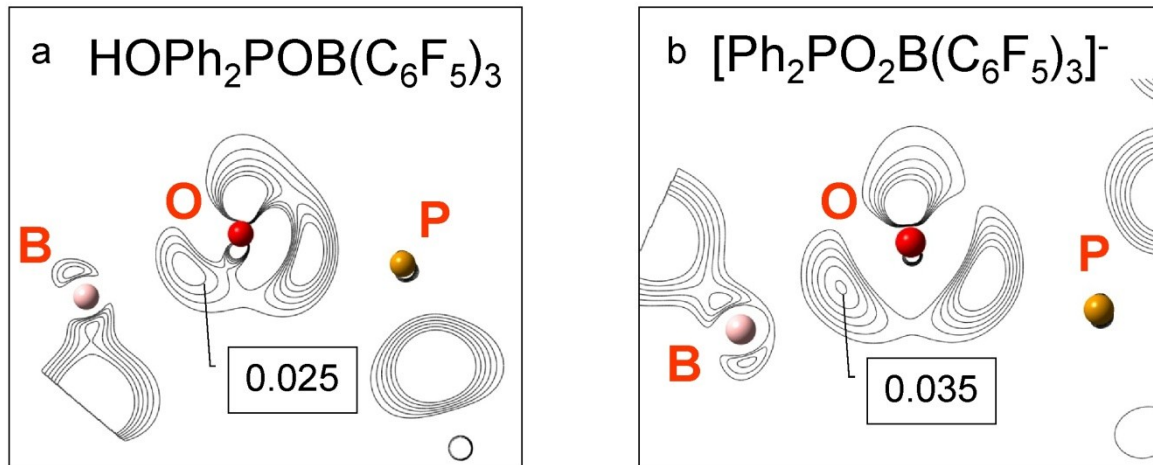


Figure S36. Profiles of the positive deformation electron density (0.010-0.0035 a.u., step 0.005 a.u.) for $(\text{C}_6\text{F}_5)_3\text{BOPPh}_2\text{OH}$ (a) and the $[\text{Ph}_2\text{P}(\text{O})\text{B}(\text{C}_6\text{F}_5)_3]^-$ ion (b) in the POB plane.

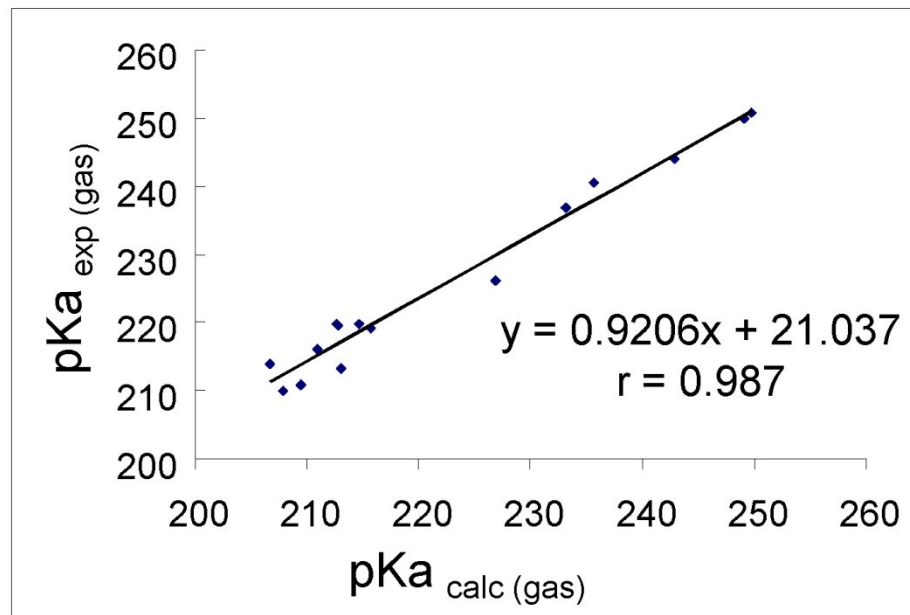


Figure S37. Linear regression between the gas-phase experimental^[S12a] and calculated pKa values.

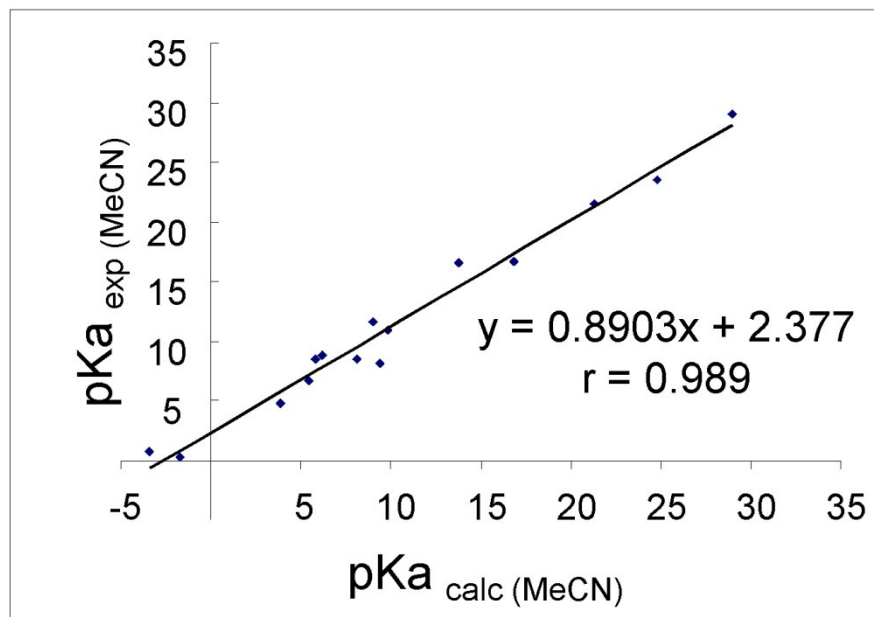


Figure S38. Linear regression between the experimental^[S12b-c,3] and calculated pKa values in MeCN solution.

Additional References

- [S1] (a) A. G. Massey and A. J. Park *J. Orgomet. Chem.* **1964**, *2*, 245. (b) M. Kuprat, M. Lehmann, A. Schulz and A. Villinger *Organometallics* **2010**, *29*, 1421.
- [S2] A. Marcó, R. Compañó, R. Rubio and I. Casals *Microchim. Acta* **2003**, *142*, 13.
- [S3] (a) G. M. Sheldrick *Acta Cryst.* **2008**, *A64*, 112. (b) L. J. Farrugia *Appl. Cryst.* **1999**, *32*, 837.
- [S4] Brandenburg, K. DIAMOND version 3.2i, Crystal Impact GbR, Bonn Germany **2012**.
- [S5] TOPAS V4: General profile and structure analysis software for powder diffraction data. Bruker AXS, Karlsruhe, Germany **2008**.
- [S6] *Gaussian 09, Revision B.01*, M. J. Frisch, G. W. Trucks, H. B. Schlegel, G. E. Scuseria, M. A. Robb, J. R. Cheeseman, G. Scalmani, V. Barone, B. Mennucci, G. A. Petersson, H. Nakatsuji, M. Caricato, X. Li, H. P. Hratchian, A. F. Izmaylov, J. Bloino, G. Zheng, J. L. Sonnenberg, M. Hada, M. Ehara, K. Toyota, R. Fukuda, J. Hasegawa, M. Ishida, T. Nakajima, Y. Honda, O. Kitao, H. Nakai, T. Vreven, J. A. Montgomery, Jr., J. E. Peralta, F. Ogliaro, M. Bearpark, J. J. Heyd, E. Brothers, K. N. Kudin, V. N. Staroverov, R. Kobayashi, J. Normand, K. Raghavachari, A. Rendell, J. C. Burant, S. S. Iyengar, J. Tomasi, M. Cossi, N. Rega, J. M. Millam, M. Klene, J. E. Knox, J. B. Cross, V. Bakken, C. Adamo, J. Jaramillo, R. Gomperts, R. E. Stratmann, O. Yazyev, A. J. Austin, R. Cammi, C. Pomelli, J. W. Ochterski, R. L. Martin, K. Morokuma, V. G. Zakrzewski, G. A. Voth, P. Salvador, J. J. Dannenberg, S. Dapprich, A. D. Daniels, Ö. Farkas, J. B. Foresman, J. V. Ortiz, J. Cioslowski, and D. J. Fox, Gaussian, Inc., Wallingford CT, **2010**.
- [S7] R. Kather, T. Svoboda, M. Wehrhahn, E. Rychagova, E. Lork, L. Dostál, S. Ketkov and J. Beckmann, *Chem. Commun.* **2015**, *51*, 5932.
- [S8] R.F.W. Bader, *Atoms in Molecules: A Quantum Theory*, Oxford University Press, Oxford UK, 1990; b) F. Cortes-Guzman and R.F.W. Bader, *Coord. Chem. Rev.* **2005**, *249*, 633.
- [S9] AIMAll (Version 13.05.06), T.A. Keith, TK Gristmill Software, Overland Park KS, USA, **2013**, <http://aim.tkgristmill.com>.
- [S10] (a) T. Lu and F. Chen, *J. Comp. Chem.* **2012**, *33*, 580. (b) T. Lu and F. Chen, *J. Mol. Graph. Model.* **2012**, *38*, 314.
- [S11] A. V. Marenich, C. J. Cramer and D. G. Truhlar *J. Phys. Chem. B* **2009**, *113*, 6378.
- [S12] (a) E. Bartmess, in: NIST Chemistry WebBook, *NIST Standard Reference Database Number 69*, Eds. P.J. Linstrom and W.G. Mallard, NIST, Gaithersburg MD, 20899,

<http://webbook.nist.gov>. (b) A. Kütt, I. Leito, I. Kaljurand, L. Soovali, V.M. Vlasov, L.M. Yagupolskii and I.A. Koppel *J. Org. Chem.* **2006**, *71*, 2829. (c) A. Kutt, T. Rodima, J. Saame, E. Raamat, V. Maemets, I. Kaljurand, I. A. Koppel, R. Yu. Garlyauskayte, Y. L. Yagupolskii, L. M. Yagupolskii, E. Bernhardt, H. Willner and I. Leito, *J. Org. Chem.* **2011**, *76*, 391.

- [S13] K. S. Alongi and G. C. Shields In: *Annual Reports in Computational Chemistry (Volume 6)*, Ed. R.A. Wheeler, Elsevier, **2010**, 113.
- [S14] (a) E. Raamat, K. Kaupmees, G. Ovsjannikov, A. Trummal, A. Kutt, J. Saame, I. Koppel, I. Kaljurand, L. Lipping, T. Rodima, V. Pihl, I.A. Koppel and I. Leito *J. Phys. Org. Chem.* **2013**, *26*, 162. (b) J. Ho, A. Klamt and M. Coote, *J. Phys. Chem. A* **2010**, *114*, 13442.
- [S15] K. A. Lyssenko, G. V. Grintselev-Knyazev and M. Yu. Antipin *Mendeleev Commun.* **2002**, *12*, 128.
- [S16] J. Guo, W.-K. Wong and W.-Y. Wong *Polyhedron* **2005**, *24*, 927.
- [S17] A. Peters, U. Wild, O. Hübner, E. Kaifer and H.-J. Himmel *Chem. Eur. J.* **2008**, *14*, 7813.